PHYSICAL REVIEW B VOLUME 44, NUMBER 17 1 NOVEMBER 1991-I

Coupled-cluster treatments of correlations in quantum antiferromagnets

R. F. Bishop, J. B. Parkinson, and Yang Xian
Department of Mathematics, The University of Manchester Institute of Science and Technology, P.O. Box 88, Manchester M60 1QD, England
(Received 20 March 1991)

The coupled-cluster method (CCM) is applied to anisotropic-quantum-antiferromagnetic models in one and two dimensions (1D and 2D). Several hierarchical approximation schemes of the CCM are defined, which are specialized for the spin-lattice models. Good results are obtained for both ground-state and excited-state energies. The spin-spin correlation functions and the staggered magnetizations are also calculated. We have found that the CCM gives a qualitatively correct description of the entire Heisenberg-Ising phase, *including* the critical point where a phase transition occurs in 1D. Some interesting differences between 1D and 2D models near the critical point are discussed.

I. INTRODUCTION

The coupled-cluster method (CCM) has proved to be one of the most powerful and universal techniques in quantum many-body theory.[1–9] Among its main advantages are its automatic avoidance of unphysical divergences in the thermodynamic limit and its systematic ability to be taken to arbitrary accuracy. The CCM has been applied to a wide range of physical systems, including problems in nuclear physics, both for finite[5,10] and infinite nuclear matter;[11] atomic and molecular systems in quantum chemistry;[3,9,12] and the electron liquids.[4,13] More recently, the CCM has also been successfully applied to the problems of the quantum anharmonic oscillator treated as a field theory in $(0+1)$ dimensions,[14] and of the Φ^4 relativistic quantum field theory.[15]

The recent discovery of the high-temperature superconductors has brought a huge resurgence of interest in strongly correlated electronic systems. Among the various model systems proposed, the two-dimensional (2D) Hubbard model is widely believed to contain the essential correlations of the active electrons in this large class of ceramic materials. The antiferromagnetic Heisenberg model can be derived from the Hubbard model at half-filling, and this is believed to describe correctly the electronic properties of the high-T_c materials before doping. By now, a large number of experiments[16] has confirmed this point, which was first suggested by Anderson[17] shortly after their discovery. In view of the successful applications of the CCM to the wide range of physical systems mentioned above, we consider it very timely and useful to apply it to study these strongly correlated models at a fundamental and microscopic level. Specifically, we study the spin-$\frac{1}{2}$ anisotropic antiferromagnetic Hamiltonian, or XXZ model. The Heisenberg model is just the isotropic point of the XXZ model. In the one-dimensional (1D) case, the spin-$\frac{1}{2}$ XXZ model has an exact solution given by the Bethe ansatz,[18] with which we can compare our results.

A recent paper by Roger and Hetherington[19] has pioneered the CCM treatment of quantum spin lattices, although their treatment was restricted to ground-state energies. In particular, they considered the Heisenberg antiferromagnetic models in 1D and 2D, and obtained good results for the ground-state energies at low levels of truncations. In this article, we wish to demonstrate that the CCM can be applied to a generic spin-lattice model and can therefore be used to study possible quantum phase transitions systematically. The XXZ model is very suitable for this purpose. We define several hierarchial approximation schemes within the CCM, specialized for the lattice models, and then systematically apply these different schemes in an attempt to improve our results. In addition to accurate values for both the ground- and excited-state energies, we find that the CCM gives a quantum phase transition in 1D and possibly also in 2D at some critical value of the anisotropy, even at a relatively low level of approximation. The phase transition shows up in the asymptotic behavior of both the staggered magnetization and the correlation functions, as well as the excitation energy gap. A brief report of some of our results has already been published.[20]

The outline of this article is as follows. Some rigorous results of the XXZ model are briefly reviewed in Sec. II, especially those exact results obtainable from the Bethe ansatz in 1D with which our results are to be compared. In Sec. III we begin with a brief summary of the coupled-cluster method, emphasizing the fact that the Hilbert space is biorthogonal in the CCM, rather than having the usual orthogonal basis in other theories. Therefore, the ket and bra states are, in general, not manifestly Hermitian conjugate to one another within any given approximation scheme of the CCM, and have to be calculated separately. We then define various approximation schemes especially tailored for the lattice models. In Secs. IV and V, we employ these schemes to calculate the ground ket state and obtain the ground-state energies in 1D and 2D, respectively. We also discuss the nature of these schemes and their physical implications. The bra states are calculated in Sec. VI.

With both ket and bra states known, we then calculate two physical quantities, namely, spin-spin correlation

functions and staggered magnetizations. For one of the approximation schemes, which contains long-range contributions, we are able to demonstrate that the correlation functions change their asymptotic behavior from exponential decay at large anisotropy to algebraic decay at some critical value of the anisotropy. We find that the staggered magnetization goes to zero in 1D and to a finite value in 2D at the respective critical points. This behavior strongly suggests the occurrence of a quantum phase transition, although there are some different features between the 1D and 2D models. As a final piece of evidence for the claimed phase transition, we calculate the excitation spectra in both 1D and 2D in Sec. VII. As expected, the energy spectra show finite gaps at large anisotropies and becomes gapless precisely at the critical point. We conclude this article with a summary and discussion in Sec. VIII.

II. BRIEF REVIEW OF SOME RIGOROUS RESULTS FOR *XXZ* MODELS

Quantum antiferromagnetic models have been of great interest in physics long before the discovery of high-temperature superconductors. As early as 1931, Bethe[18] had found the exact solutions for the eigenstates of the 1D spin-$\frac{1}{2}$ Heisenberg antiferromagnetic model. Seven years later, Hulthén[21] calculated the exact value of the ground-state energy based on the Bethe ansatz. Since then the Bethe ansatz has been generalized to the *XXZ* model[22] and also to other 1D quantum systems.[23] The excitations and other physical properties of the corresponding models have also been investigated by the Bethe ansatz and other means within approximately the last 30 years.[24] In particular, for the *XXZ* model, the staggered magnetization was obtained by Baxter[25] in 1973, and the asymptotics of the correlation functions were obtained in 1986 by the algebraization of the Bethe ansatz, namely, the quantum inverse-scattering method (QISM).[26] The QISM has confirmed the results of earlier work by Luther and Peschel.[27]

The nearest-neighbor-coupling *XXZ* model Hamiltonian is given in any number of dimensions, and in terms of the spin operator $\mathbf{s}\equiv\{s^\alpha;\ \alpha=x,y,z\}$, by

$$H=\tfrac{1}{2}\sum_{l,\rho}(s_l^x s_{l+\rho}^x+s_l^y s_{l+\rho}^y+\Delta s_l^z s_{l+\rho}^z)\ , \tag{2.1}$$

where the index l runs over all N lattice sites, the index ρ denotes the z nearest-neighbor sites, and we have imposed the periodic boundary condition and set the antiferromagnetic coupling constant and the lattice spacing to unity. We shall consider only bipartite lattices with even N, so that each sublattice contains $\frac{1}{2}N$ spins. The Heisenberg model corresponds to the isotropic case, i.e., $\Delta=1$, while the *XY* model is given by $\Delta=0$. The Hamiltonian of Eq. (2.1) commutes with the z component of total spin, $s^z_{\text{total}}(\equiv\sum_l s_l^z)$, which is therefore a good quantum number. We shall be interested particularly in those values of Δ for which the ground state is antiferromagnetic, and hence lies in the subspace, $s^z_{\text{total}}=0$.

First, we discuss the two-dimensional case of the square lattice. Despite great efforts, few rigorous results are known. Specifically, there is no rigorous result for whether the ground state of the Hamiltonian of Eq. (2.1) at $\Delta=1$ and $s=\frac{1}{2}$ on a 2D square lattice possesses a long-range order (LRO) of the Ising type, although most of the approximate calculations do show a finite LRO with a staggered magnetization of about two-thirds of the Ising value (see Ref. 28 and references therein). Perhaps the closest rigorous argument in this respect is provided by Kubo and Kishi.[29] They apply various sum rules for the *XXZ* model and have shown that, for $s=\frac{1}{2}$, the ground state possesses an off-diagonal LRO akin to that of the *XY*-like state at small anisotropy ($0<\Delta<0.13$), and a diagonal LRO akin to that of the Ising-like state at large anisotropy ($\Delta>1.78$). Unfortunately, their proof cannot directly be extended to the most interesting point, namely the isotropic Heisenberg model with $\Delta=1$.

In contrast to the 2D case, the 1D spin-$\frac{1}{2}$ *XXZ* model can be solved exactly by the Bethe ansatz, as stated above. We summarize below the main exact results for the 1D spin-$\frac{1}{2}$ *XXZ* model. In the ferromagnetic regime ($\Delta\le-1$), the exact ground state has all of the spins aligned in the same direction and its energy is trivially given by

$$\frac{E_g}{N}=\frac{1}{4}\Delta,\quad \Delta\le-1\ . \tag{2.2}$$

Precisely at the point $\Delta=-1$, the system undergoes a first-order phase transition to the so-called critical antiferromagnetic phase where the spin-spin correlation function shows algebraic decaying behavior, details of which are given below. This phase covers the entire range of $|\Delta|\le1$. Its exact ground-state energy is

$$\frac{E_g}{N}=\tfrac{1}{4}\cos\theta-\tfrac{1}{2}\sin^2\theta\int_{-\infty}^{\infty}\frac{d\omega}{\cosh(\pi\omega)[\cosh(2\theta\omega)-\cos\theta]}\ ,\quad |\Delta|\le1\ , \tag{2.3}$$

where $0\le\theta\equiv\arccos\Delta\le\pi$. From Eq. (2.3) one can evaluate the energy values at various special points. Thus, at $\Delta=-1$, $E_g/N=-\frac{1}{4}$; at $\Delta=0$ (i.e., the *XY* model), $E_g/N=-1/\pi$; and at the isotropic point $\Delta=1$ (i.e., the Heisenberg model), $E_g/N=\frac{1}{4}-\ln2$. The corresponding spin-wave excitation spectrum in this critical region is gapless and given by

$$E_q=\frac{\pi}{2}\left[\frac{\sin\theta}{\theta}\right]\sin q,\quad 0\le q\le\pi\ . \tag{2.4}$$

From this region, the system undergoes another phase transition at $\Delta=1$ to the Ising-like phase which exists for all $\Delta>1$. This transition is second order and the ground-state energy changes continuously and smoothly at the critical point. For $\Delta\ge1$ the ground-state energy is given by

$$\frac{E_g}{N}=\tfrac{1}{4}\cosh\gamma - \tfrac{1}{2}\sinh\gamma\left[1+4\sum_{m=1}^{\infty}[1+\exp(2m\gamma)]^{-1}\right], \quad \Delta\geq 1 , \tag{2.5}$$

where $\Delta\equiv\cosh\gamma$. Direct evaluation from Eq. (2.5) shows that, in the Heisenberg limit ($\Delta=1$), the energy has the same value as given by Eq. (2.3), whereas in the Ising limit ($\Delta\to\infty$) one has

$$\frac{E_g}{N}\to-\frac{1}{4}\left[\Delta+\frac{1}{\Delta}\right], \quad \Delta\to\infty . \tag{2.6}$$

In this Ising-like region ($\Delta>1$), the spin-wave spectrum has a finite gap, and the excitation energy is given by

$$E_q=\frac{K_1}{\pi}\sinh\gamma\sqrt{1-k_1^2\cos^2 q}, \quad \Delta\equiv\cosh\gamma , \tag{2.7}$$

where the constant k_1 is given in terms of the two complete elliptic integrals K_1 and K_1',

$$K_1\equiv\int_0^{\pi/2}d\theta\frac{1}{\sqrt{1-k_1^2\sin^2\theta}} , \qquad K_1'\equiv\int_0^{\pi/2}d\theta\frac{1}{\sqrt{1-(1-k_1^2)\sin^2\theta}} , \tag{2.8}$$

by the relation

$$\frac{K_1'}{K_1}=\frac{\gamma}{\pi} . \tag{2.9}$$

Faddeev and Takhtajan[24] have pointed out that the spectra given by Eqs. (2.4) and (2.7) are unphysical single-kink excitations with spin $\frac{1}{2}$. The physical spin-wave excitations with $s^z_{\text{total}}=\pm 1$ are actually formed from two such kink solutions. The spectrum is, in fact, a continuum,[24] given by the form

$$E_q(k)=E_k+E_{q-k} . \tag{2.10}$$

Thus, the spectra given by Eqs. (2.4) and (2.7) are the lower boundaries to this continuum.

Finally, the spin-spin correlation functions and the staggered magnetization for the 1D lattice are defined by, respectively,

$$G^{\alpha\beta}(n)\equiv\frac{1}{s^2}\langle s_l^\alpha s_{l+n}^\beta\rangle, \quad M^\alpha\equiv\frac{1}{s}|\langle s_l^\alpha\rangle| , \tag{2.11}$$

with $\alpha,\beta=x,y,z$, and where s is the spin quantum number, $s^2=s(s+1)$. Because of the translational invariance of the lattice systems, both $G(n)$ and M^α are independent of the index l in Eq. (2.11). The asymptotic value of the magnitude of $G^{zz}(n)$ as $n\to\infty$ is equal to the square of the staggered magnetization M^z.

In the critical region ($|\Delta|\leq 1$), there is no diagonal LRO, i.e., $M^z=0$, and the leading asymptotes of the correlation functions have power-law decay behavior as $n\to\infty$,[26]

$$G^{zz}(n)\to\begin{cases}A_1/n^2, & -1<\Delta<0 ,\\ (-1)^n B_1/n^{\pi/\theta'}, & 0<\Delta\leq 1 ,\end{cases} \tag{2.12}$$

where A_1 and B_1 are constants which depend on Δ, and the exponent $\pi/2\leq\theta'\equiv\arccos(-\Delta)\leq\pi$.

For $\Delta>1$, the absolute magnitude of $G^{zz}(n)$ decays exponentially to a nonzero value, the square of the order parameter M^z. Very near the critical point $\Delta_c=1$, M^z as a function of Δ shows the essential singularity behavior[25]

$$M^z\to\text{const}\times\sqrt{\Delta-1}\exp\left[-\frac{C_1}{\sqrt{\Delta-1}}\right], \quad \Delta\to 1^+ , \tag{2.13}$$

where C_1 is a positive constant. The energy gap in this Ising-like region, given by Eqs. (2.7)–(2.9), also shows an essential singularity as

$$E_{q=0}\to\text{const}\times\exp\left[-\frac{C_1'}{\sqrt{\Delta-1}}\right], \quad \Delta\to 1^+ , \tag{2.14}$$

where C_1' is another positive constant.

The exact 1D ground-state energy for a range of values of Δ which spans all of the phases is shown later in Fig. 2, along with our CCM results. The corresponding exact staggered magnetization for $\Delta\geq 1$ is also shown later in Fig. 6.

III. GROUND KET STATE

We begin this section with a brief summary of the CCM, taking our spin model on a bipartite lattice as example. For more detailed reviews, the interested reader is referred to Refs. 4–10.

The first step of the CCM is to choose a model state $|\Phi\rangle$. Although it is not necessary to do so, an uncorrelated state is often taken. For our antiferromagnetic model, the N-body Néel state is the obvious choice, consisting of two alternating sublattices, with their spins in the $\pm z$ directions, respectively. The exact ground ket state $|\Psi\rangle$ is quite generally expressed in the CCM form as

$$|\Psi\rangle=e^S|\Phi\rangle , \tag{3.1}$$

where the correlation operator S is partitioned into one-body, two-body, etc., and up to N-body pieces with N the total number of spins in the system. We choose N to be an even number. In particular, one writes

$$S=\sum_{n=1}^{N}S_n , \tag{3.2}$$

with S_n expressed in terms of n-fold "creation" operators,

$$S_n=\sum_{i_1,i_2,\ldots,i_n}\mathcal{S}_{i_1 i_2\cdots i_n}C_{i_1}^+C_{i_2}^+\ldots C_{i_n}^+ . \tag{3.3}$$

These creation operators C_i^+ are defined according to the Hamiltonian of the system and with respect to the chosen model state. In our spin model, the creation operators C_i^+ are defined by the spin-flip operators with respect to the Néel model state, i.e., the spin-raising operators s_i^+

for the down-spin sublattice, and the spin-lowering operators s_j^- for the up-spin sublattice. It should be noted that, by definition, each term in Eq. (3.3) commutes with every other term.

The CCM Schrödinger ground-state equation is then written in the following form:

$$He^S|\Phi\rangle = E_g e^S|\Phi\rangle \ , \tag{3.4}$$

or in the equivalent similarity-transformed form,

$$e^{-S}He^S|\Phi\rangle = E_g|\Phi\rangle \ . \tag{3.5}$$

Taking the inner product firstly with the model state $\langle\Phi|$, one has the expression for the energy

$$E_g = \langle\Phi|e^{-S}He^S|\Phi\rangle \ , \tag{3.6}$$

and secondly with the state $\langle\Phi|C_{i_1}^- C_{i_2}^- \ldots C_{i_n}^-$, one has a set of *nonlinear coupled* equations for the coefficients $\mathcal{S}_{i_1 i_2 \ldots i_n}$ in Eq. (3.3):

$$\langle\Phi|C_{i_1}^- C_{i_2}^- \ldots C_{i_n}^- e^{-S}He^S|\Phi\rangle = 0, \quad n = 1,2,\ldots,N \ , \tag{3.7}$$

where the destruction operators C_i^- are the Hermitian adjoints of the corresponding creation operators C_i^+. These nonlinear coupled equations are the hallmark of the CCM. One can also use the fact that the similarity-transformed Hamiltonian $e^{-S}He^S$ can be written in terms of nested commutators using the well-known expansion

$$e^{-S}He^S = H + [H,S] + \frac{1}{2!}[[H,S],S] + \ldots \ . \tag{3.8}$$

This otherwise infinite expansion always terminates after a finite number of terms in our case because the Hamiltonian H contains a finite number of destruction operators. For example, for a Hamiltonian with a two-body potential, the expansion terminates at fourth order.

Before we apply the CCM to calculate the ground ket state of the *XXZ* model, we transform the model Hamiltonian of Eq. (2.1) into a more convenient form. First, we perform a notational rotation[19] of 180° about the y axis of one sublattice of the Néel state so that all spins in the model state align in the same direction, say down, i.e., along the $-z$ axis. This is equivalent to the transformation $s_x \to -s_x$, $s_y \to s_y$, and $s_z \to -s_z$ on the up sublattice.

Secondly, because we are concerned only with spin-$\frac{1}{2}$ models here, we use the Pauli matrices to replace the spin operators,

$$\sigma^\alpha \equiv 2s^\alpha, \quad \alpha = x,y,z \ . \tag{3.9}$$

We thus equivalently define raising and lowering operators by

$$\sigma_i^\pm \equiv \tfrac{1}{2}(\sigma_i^x \pm i\sigma_i^y) \tag{3.10}$$

for the down-spin sublattice and

$$\sigma_j^\pm \equiv \tfrac{1}{2}(-\sigma_j^x \pm i\sigma_j^y) \tag{3.11}$$

for the rotated up-spin sublattice. We note that the sublattice rotation leaves the commutation relations of the Pauli matrices unchanged,

$$\begin{aligned} &[\sigma_l^+, \sigma_{l'}^-] = \sigma_l^z \delta_{ll'} \ , \\ &[\sigma_l^z, \sigma_{l'}^\pm] = \pm 2\sigma_l^\pm \delta_{ll'} \ . \end{aligned} \tag{3.12}$$

The *XXZ* model Hamiltonian of Eq. (2.1) in our rotated Néel basis is now given by

$$H = -\tfrac{1}{4}\sum_{l,\rho}\left[\frac{\Delta}{2}\sigma_l^z\sigma_{l+\rho}^z + \sigma_l^+\sigma_{l+\rho}^+ + \sigma_l^-\sigma_{l+\rho}^-\right] . \tag{3.13}$$

The n-body operators S_n of Eq. (3.3) in our model are then written as

$$S_n = C_n \sum_{l_1,l_2,\ldots,l_n} \mathcal{S}_{l_1 l_2 \ldots l_n}\sigma_{l_1}^+\sigma_{l_2}^+ \ldots \sigma_{l_n}^+ \ , \tag{3.14}$$

where C_n is some suitable normalization constant. Noting that the ground state of the antiferromagnetic spin models is in the subspace of $s_{\text{total}}^z = 0$, it follows that the correlation operator S should contain only those partitions S_n with even n, and with $n/2$ creation operators on each of the two sublattices. From now on, to avoid confusion, we shall exclusively use indices i or $\{i_n\}$ for one sublattice, and j or $\{j_n\}$ for the other. Hence, one can rewrite Eq. (3.14) with a rather natural choice of the normalization constant C_n as

$$S_{2n} = \frac{1}{(n!)^2}\sum_{i_1,i_2,\ldots,i_n}\sum_{j_1,j_2,\ldots,j_n}\mathcal{S}_{i_1 i_2 \ldots i_n; j_1 j_2 \ldots j_n}\sigma_{i_1}^+\sigma_{i_2}^+ \ldots \sigma_{i_n}^+\sigma_{j_1}^+\sigma_{j_2}^+ \ldots \sigma_{j_n}^+ \ , \tag{3.15}$$

where an arbitrary coefficient $\mathcal{S}_{i_1 \ldots i_n; j_1 \ldots j_n}$ with any repeated index may be taken to be identically zero because of the property of the Pauli matrices, $(\sigma^+)^2 = 0$. This is only true for the spin-$\frac{1}{2}$ systems considered here.

As in any microscopic theory, one needs to make a truncation approximation in a practical calculation. In other words, we shall need to truncate the total possible number of cluster configurations in Eqs. (3.2) and (3.15) for the correlation operator S to some finite or infinite subset. We shall discuss several physically motivated such approximations below. In each such case, the CCM equations are derived from Eq. (3.7) with the destruction operators chosen, in turn, to be the Hermitian adjoints of the creation operators corresponding to each configuration retained in the approximation for S. We thus have a set of equations equal in number to the cluster coefficients retained.

The most common truncation scheme of the CCM is the so called SUBn approximation in which one only keeps up to the n-body correlations,

$$S \rightarrow S_{\mathrm{SUB}n} = \sum_{l=1}^{n/2} S_{2l} \ , \tag{3.16}$$

and where in the present case n is an even positive integer. Therefore, for example, the SUB4 approximation consists of two sets of coupled equations, namely the two-spin-flip and four-spin-flip equations. They are obtained, respectively, as follows:

$$\langle \Phi | \bar{\sigma_i} \bar{\sigma_j} \exp(-S_{\mathrm{SUB4}}) H \exp(S_{\mathrm{SUB4}}) | \Phi \rangle = 0 \ ,$$

or

$$\sum_{\rho} \left[(1+2\Delta \mathcal{S}_{i;i+\rho}+2\mathcal{S}_{i;i+\rho}^2)\delta_{i+\rho,j} - 2(\Delta+2\mathcal{S}_{i;i+\rho})\mathcal{S}_{i;j} + \sum_{i'} (\mathcal{S}_{i';j}\mathcal{S}_{i;i'+\rho}+\mathcal{S}_{ii';i'+\rho,j}) \right] = 0 \ ; \tag{3.17}$$

and

$$\langle \Phi | \bar{\sigma_i} \bar{\sigma_{i'}} \bar{\sigma_j} \bar{\sigma_{j'}} \exp(-S_{\mathrm{SUB4}}) H \exp(S_{\mathrm{SUB4}}) | \Phi \rangle = 0 \ ,$$

or

$$\begin{aligned}
\sum_{\rho} \Big[& (2-\delta_{i+\rho,j}-\delta_{i+\rho,j'}-\delta_{i'+\rho,j}-\delta_{i'+\rho,j'})\Delta\mathcal{S}_{ii';jj'} - \Delta\mathcal{S}_{i;j'}\mathcal{S}_{i';j}(\delta_{i+\rho,j}+\delta_{i'+\rho,j'}) \\
& - \Delta\mathcal{S}_{i;j}\mathcal{S}_{i';j'}(\delta_{i+\rho,j'}+\delta_{i'+\rho,j}) + \mathcal{S}_{i;j}(\mathcal{S}_{ii';i+\rho,j'}+\mathcal{S}_{j-\rho,i';jj'}) \\
& + \mathcal{S}_{i;j'}(\mathcal{S}_{ii';i+\rho,j}+\mathcal{S}_{j'-\rho,i';jj'}) + \mathcal{S}_{i';j}(\mathcal{S}_{ii';i'+\rho,j'}+\mathcal{S}_{j-\rho,i;jj'}) \\
& + \mathcal{S}_{i';j'}(\mathcal{S}_{ii';i'+\rho,j}+\mathcal{S}_{j'-\rho,i;jj'}) - 2(\delta_{i+\rho,j}+\delta_{i+\rho,j'}+\delta_{i'+\rho,j}+\delta_{i'+\rho,j'}-2)\mathcal{S}_{i;i+\rho}\mathcal{S}_{ii';jj'} \\
& + \mathcal{S}_{i;j}(\mathcal{S}_{i;j'}\mathcal{S}_{i';i+\rho}+\mathcal{S}_{i';j}\mathcal{S}_{j-\rho;j'}) + \mathcal{S}_{i';j'}(\mathcal{S}_{i';j}\mathcal{S}_{i;i'+\rho}+\mathcal{S}_{i;j'}\mathcal{S}_{j'-\rho;j}) \\
& - 2\mathcal{S}_{i;i+\rho}[\mathcal{S}_{i;j}\mathcal{S}_{i';j'}(\delta_{i+\rho,j'}+\delta_{i'+\rho,j}) + \mathcal{S}_{i;j'}\mathcal{S}_{i';j}(\delta_{i+\rho,j}+\delta_{i'+\rho,j'})] \\
& - \tfrac{1}{2}\sum_{i''} (\mathcal{S}_{i'';j}\mathcal{S}_{ii',i''+\rho,j'}+\mathcal{S}_{i'';j'}\mathcal{S}_{ii';i''+\rho,j}+\mathcal{S}_{i;i''\rho}+\mathcal{S}_{i''i';jj'}+\mathcal{S}_{i';i''+\rho}\mathcal{S}_{ii'';jj'}) \Big] = 0 \ .
\end{aligned} \tag{3.18}$$

We note that Eqs. (3.17) and (3.18) are valid within the SUB4 approximation for a bipartite lattice in an arbitrary number of dimensions.

The ground-state energy is obtained from Eq. (3.6) as

$$\frac{E_g}{N} = -\frac{z}{8}(\Delta+2b_1) \ , \tag{3.19}$$

where z is the coordination number (i.e., the number of nearest neighbors) of the bipartite lattice, and $b_1 \equiv \mathcal{S}_{i;i+\rho}$ is the first two-body coefficient. We note that Eq. (3.19), which is exact and not just restricted to the SUB4 approximation, gives the ground-state energy in terms of the single lowest-order correlation coefficient b_1 under any approximation. Clearly the first term, $-z\Delta/8$, in Eq. (3.19) is just the classical Néel value, and the term involving b_1 gives the correction to this classical value due to quantum fluctuations.

Other physically motivated truncation schemes are also possible. We have found several useful ones defined as follows. Thus, a second sequence of approximations is based on the localized nature of the interaction itself, which we call the LSUBn scheme where the character L stands for "locale." At the LSUBn level of approximation, one retains only those configurations in the correlation operator S which contain any number of spin flips with respect to the Néel state over a locale or localized region of n contiguous sites, and which are compatible with the restriction $s^z_{\mathrm{total}}=0$.

A third sequence of approximations is motivated by the kink structures of the spin systems in 1D, or by the domain structure in a dimension more than one. We call it the PSUBn scheme with P standing for "plaquette." By definition, each plaquette consists of one contiguous cluster of arbitrary size in which all of the spins are flipped with respect to the Néel state. Hence the PSUBn approximation will contain configurations with up to n such plaquettes.

Finally, a fourth sequence of truncation schemes is a combination of the SUBn and LSUBm schemes (with $m > n$), hence denoted as SUBn + LSUBm. This scheme not only contains the arbitrarily long-range contributions of the SUBn configurations but also the localized higher-order m-body correlations (with $m > n$) of the LSUBm configurations which are relatively easy to handle. This scheme in our calculations is the most promising one because it gives a phase transition as well as accurate numerical values of the ground-state energies as we shall see shortly.

IV. GROUND-STATE ENERGY IN 1D

In this section we shall study separately the various truncation schemes defined in Sec. III for the 1D model and leave the corresponding calculations for the 2D model to the next section.

TABLE I. Ground-state energy per spin for the 1D XXZ model at several values of Δ under various SUB2-m schemes. The full SUB2 ($\equiv$SUB2-∞) results and the exact results of Ref. 22 are given in the last two columns.

Δ	SUB2-2	SUB2-4	SUB2-6	SUB2-8	SUB2-∞	Exact
5.0	−1.2986	−1.2986	−1.2986	−1.2986	−1.2986	−1.2995
2.0	−0.6076	−0.6078	−0.6079	−0.6079	−0.6079	−0.6172
1.0	−0.4167	−0.4186	−0.4186	−0.4186	−0.4186	−0.4432
0.5	−0.3421	−0.3494	−0.3504	−0.3506	−0.3506	−0.3750

A. SUBn scheme

In Eq. (3.17) we obtain the equations of the full SUB2 approximation by setting all four-body coefficients to zero. Using the translational invariance, we write $\mathcal{S}_{i;i+r} \equiv b_r = b_{-r}$, where r is a lattice vector which connects the two sublattices of the Néel model state. In 1D, r is thus a positive or negative odd integer, and the full SUB2 equations then become

$$\sum_{\rho} \left[(1+2\Delta b_1 + 2b_1^2)\delta_{\rho,r} - 2(\Delta + 2b_1)b_r + \sum_{r'} b_{r'+\rho+1} b_{r-r'-1} \right] = 0 , \tag{4.1}$$

where $\rho = \pm 1$ denotes the nearest-neighbor lattice vectors in 1D, and the sum on r' runs over all (positive and negative) odd integers.

One can define a partial SUB2 approximation here which we call the SUB2-m scheme. In this SUB2-m approximation, one keeps only those coefficients b_r with $|r| < m$. For example, the lowest approximation of all is the SUB2-2 truncation in which one keeps only the single independent coefficient b_1. The SUB2-4 approximation retains the two independent coefficients, b_1 and b_3, and the SUB2-6 approximation retains the three independent coefficients, b_1, b_3, and b_5, etc.

The SUB2-2 equation is easy to solve. In Eq. (4.1), setting all other coefficients to zero, one has a second-order equation for b_1,

$$1 - 2\Delta b_1 - 3b_1^2 = 0 \tag{4.2}$$

with solution

$$b_1 = \tfrac{1}{3}(\sqrt{\Delta^2+3} - \Delta) , \tag{4.3}$$

where we have discarded the other unphysical solution. At $\Delta = 1$ (the Heisenberg model) and $\Delta = 0$ (the XY model), the ground-state energies are obtained respectively, from Eq. (3.19) as $E_g/N = -\frac{5}{12} \approx -0.417$ and $E_g/N = -\sqrt{3}/6 \approx -0.289$. This compares with the exact results of -0.443 and -0.318, respectively, from Sec. II, to the same three significant figure level of accuracy. From Eqs. (4.3) and (3.19) it is easy to see that the SUB2-2 approximation gives the same asymptotic form for the ground-state energy in the Ising limit ($\Delta \to \infty$) as that of the exact result, given by Eq. (2.6). It is interesting to note that our SUB2-2 wave function has the same form as that used by Sachdev[30] in a variational calculation at $\Delta = 1$. In contrast with our own method, he minimized the expectation value of the Hamiltonian with respect to b_1 and thereby obtained a value $E_g/N \approx -0.428$.

The SUB2-m approximations with larger m show a rapid convergence in the energy calculation for most positive values of Δ. This is demonstrated in Table I and Fig. 1. In Table I we have listed the results for the ground-state energy under the various SUB2-m schemes (up to $m = 8$) at several values of Δ. We have also included the corresponding exact results from Sec. II in the last column. It is interesting to observe in Fig. 1 that, at small Δ, the energy curves from the various SUB2-m

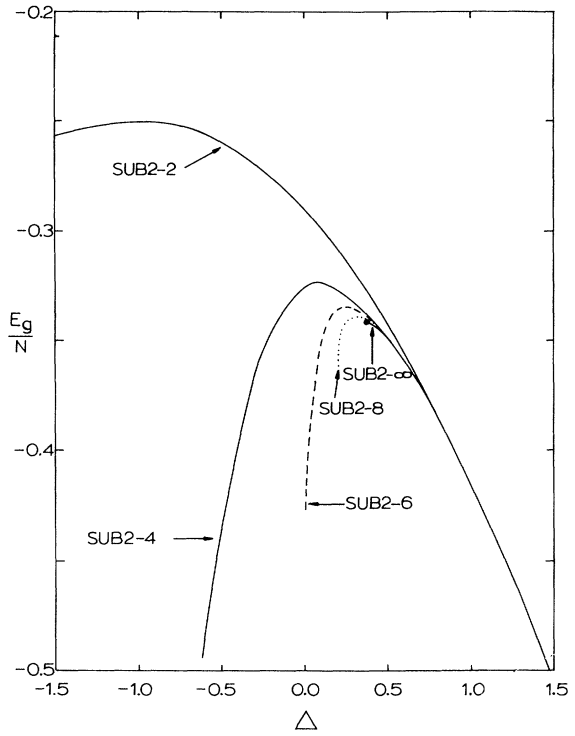

FIG. 1. Ground-state energy per spin for the 1D spin-$\frac{1}{2}$ XXZ model as a function of Δ, showing the results of several SUB2-m and the full SUB2 ($\equiv$SUB2-∞) schemes described in the text. The terminating point of the full SUB2 approximation is indicated.

schemes bend downward increasingly rapidly as m increases, indicating the possible existence of a special point in that region. This point will become more explicit when the full SUB2 equations are solved.

The complete equations of the full SUB2 approximation, Eq. (4.1), can be solved exactly by the so-called sublattice Fourier-transform method. We leave the details to Appendix A and simply give the solution here:

$$b_r=\frac{K}{\pi}\int_0^{\pi}dq\frac{\cos(rq)}{\cos(q)}(1-\sqrt{1-k^2\cos^2q}\,)\ , \tag{4.4}$$

where the constants K and k are defined by

$$K\equiv\Delta+2b_1,\quad k^2\equiv\frac{1+2\Delta b_1+2b_1^2}{(\Delta+2b_1)^2}\ . \tag{4.5}$$

In particular, b_1 is determined self-consistently by the relation

$$b_1=\frac{K}{\pi}\int_0^{\pi}dq(1-\sqrt{1-k^2\cos^2q}\,)\ . \tag{4.6}$$

In the large-Δ limit, this b_1 again gives the same asymptotic form for the ground-state energy from Eq. (3.19) as that of the exact result given by Eq. (2.6).

We note that a real solution to Eq. (4.6) ceases to exist when $k>k_c=1$. This gives the critical value

$$b_1=\alpha\Delta_c,\quad \Delta_c=\frac{1}{\sqrt{1+2\alpha+2\alpha^2}}\ , \tag{4.7}$$

where $\alpha\equiv(\pi-2)/(4-\pi)$. Numerically, $\Delta_c\approx0.3728$. The ground-state energy of this complete SUB2 approximation is shown in Fig. 2, together with that of the SUB2-2 approximation. Most interestingly, however, the behavior of b_r as a function of r in the SUB2 approximation changes its exponential decay to a power-law decay precisely at this critical point, i.e., as $r\to\infty$,

$$b_r\to\begin{cases}a/l^r, & \Delta>\Delta_c\ ,\\ b/r^2, & \Delta=\Delta_c\ ,\end{cases} \tag{4.8}$$

where b is a constant and a and $l\,(>1)$ are functions of Δ only. This behavior indicates a possible phase change at Δ_c. Further evidence for a phase change at $\Delta=\Delta_c$ will be given in Secs. VI and VII, where other physical quantities such as the order parameter, correlation functions, and the excitation spectrum are calculated.

B. LSUBn scheme

The lowest-order approximation of the LSUBn scheme is given by the LSUB2 truncation which is the same as the SUB2-2 approximation, i.e., as given in Eqs. (4.2) and (4.3).

The LSUB4 scheme retains only three independent configurations in 1D, namely the two lowest independent two-spin-flip configurations characterized by the coefficients b_1 and b_3, and the most compact four-spin-flip configuration represented by the coefficient $\mathcal{S}_{i,i+2;i+1,i+3}\equiv g_4$. Again here we use g_4 to replace the first four-body coefficient for simplicity. As always, we assume that the configuration coefficients share the obvious lattice symmetry, so that here, for example,

$$\mathcal{S}_{i,i+2;i-1,i+1}=\mathcal{S}_{i,i+2;i+3,i+1}=g_4\ ,$$

etc. In fact, one can write the correlation operator S under this LSUB4 approximation simply as (in 1D only)

$$S\to S_{\text{LSUB4}}=\sum_l(b_1\sigma_l^+\sigma_{l+1}^++b_3\sigma_l^+\sigma_{l+3}^+ +g_4\sigma_l^+\sigma_{l+1}^+\sigma_{l+2}^+\sigma_{l+3}^+)\ , \tag{4.9}$$

where the sum on l runs over all lattice sites.

The three independent coefficients of the LSUB4 approximation are now determined by three coupled equations, obtained from Eqs. (3.17) and (3.18) by setting all other coefficients to zero,

$$1-2\Delta b_1-3b_1^2+2b_1b_3+2b_3^2+2g_4=0\ , \tag{4.10a}$$

$$b_1^2-4\Delta b_3-4b_1b_3+g_4=0\ , \tag{4.10b}$$

$$-\Delta(b_1^2+2b_1b_3)+g_4(\Delta+4b_1+b_3)+2b_1b_3^2=0\ . \tag{4.10c}$$

The corresponding numerical solution for the ground-state energy is also shown in Fig. 2 for comparison. Several values for the energy at various points of Δ under this LSUB4 approximation are given in Table II. As can be seen from Fig. 2 and Table II, the LSUB4 approximation gives better results for the energy than the LSUB2

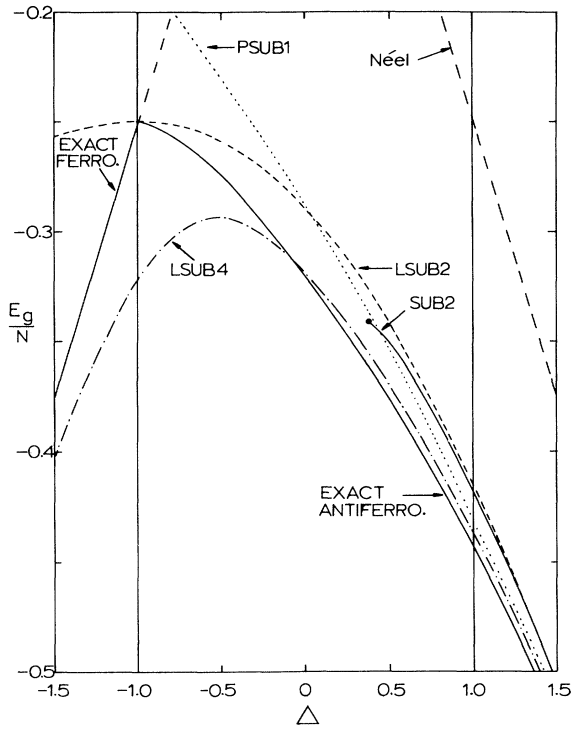

FIG. 2. Ground-state energy per spin for the 1D spin-$\frac{1}{2}$ XXZ model as a function of Δ, showing the exact results of Ref. 22, and our CCM results for the LSUB2, LSUB4, PSUB1, and full SUB2 approximation schemes described in the text. The terminating point of the full SUB2 scheme is indicated. The exact result becomes critical at $\Delta=1$, although this is not obvious from the energy plot.

TABLE II. Ground-state energy per spin for the 1D XXZ model in the LSUB4 and SUB2+LSUB4 schemes at several values of Δ, together with the exact results of Ref. 22.

Δ	5.0	2.0	1.0	0.5	0.0	−0.5
LSUB4	−1.2995	−0.6155	−0.4363	−0.3692	−0.3193	−0.2932
SUB2+LSUB4	−1.2995	−0.6155	−0.4366	−0.3727		
Exact	−1.2995	−0.6172	−0.4432	−0.3750	−0.3183	−0.2745

(≡SUB2-2) and the full SUB2 schemes for most values of Δ. At small and negative values of Δ, both LSUB4 and LSUB2 results deviate from the exact results significantly, and the LSUB4 result becomes lower than the exact one.

C. PSUBn scheme

As defined earlier, the PSUBn scheme consists of n plaquettes of contiguous flipped spins with respect to the Néel model state. Even at the lowest order of this scheme, PSUB1, up to N-body correlations have been taken into account, albeit only partially, where N is the number of particles in the system. The PSUB1 correlation operator is thus given by

$$S \rightarrow S_{\mathrm{PSUB1}} = \sum_{i=1}^{N} \sum_{m=1}^{N/2} g_{2m} \prod_{l=1}^{2m} \sigma_{i+l-1}^{+} , \tag{4.11}$$

where $g_2 \equiv b_1$. The CCM equations are given in this case by

$$1-2\Delta g_2 - 3g_2^2 + 2g_4 = 0 , \tag{4.12a}$$

$$\Delta g_{2m} - g_{2m+2} + 2m g_2 g_{2m} - \Delta \sum_{n=1}^{m-1} g_{2n} g_{2m-2n} + (1-\delta_{2,m}) \sum_{n=2}^{m-1} g_{2n} g_{2m-2n+2} = 0, \quad m \geq 2 . \tag{4.12b}$$

We have not attempted to obtain an analytic expression for the coefficients $\{g_{2m}\}$ in this scheme. However, the numerical solution gives the ground-state energy curve which is also shown in Fig. 2 for comparison.

In Table III we give the results under some partial PSUB1 approximations at several values of Δ. The definition for the partial PSUB1 approximations, PSUB1-m, is similar to that for the partial SUBn scheme. Hence, the PSUB1-2 approximation retains one coefficient g_2; PSUB1-4 retains g_2 and g_4; PSUB1-6 retains g_2, g_4, and g_6, etc. From Table III we again see that the convergence is very rapid as m increases; and from Fig. 2, one concludes that, although in this scheme partial higher-order many-body corrections are taken into account, the values for the ground-state energy obtained are not better than those in LSUB4 approximation. This is somewhat disappointing, but it clearly shows the importance of some configurations over others, at least so far as the ground-state energy is concerned.

D. SUBn +LSUBm scheme

As discussed above, the full SUB2 scheme retains only the two-spin-flip configurations. It includes the long-range contributions of two-body correlations and shows an interesting changeover in the asymptotic behavior for the coefficient b_r as $r \rightarrow \infty$. However, its result for the ground-state energy is not better than that of the LSUB4 scheme. One can improve the result of the SUB2 scheme by taking partial four-body corrections into account without much difficulty. If we consider the g_4 contribution together with those included in the full SUB2 scheme, then all the terms in the SUB2 and the LSUB4 schemes are included, i.e., SUB2+LSUB4. The resulting equations for the configuration coefficients, obtained from Eqs. (3.17) and (3.18), are now given as

$$1-2\Delta b_1 - 6b_1^2 + 2g_4 + \sum_{n=-\infty}^{\infty} b_{2n-1}(b_{2n-1}+b_{2n+1}) = 0 , \tag{4.13a}$$

TABLE III. Ground-state energy per spin for the 1D XXZ model under various PSUB1-m approximations at several values of Δ. The exact results of Ref. 22 are included in the last column.

Δ	PSUB1-2	PSUB1-4	PSUB1-6	PSUB1-8	PSUB1-10	Exact
5.0	−1.2986	−1.2994	−1.2995	−1.2995	−1.2995	−1.2995
2.0	−0.6076	−0.6144	−0.6151	−0.6152	−0.6152	−0.6172
1.0	−0.4167	−0.4297	−0.4310	−0.4311	−0.4311	−0.4432
0.0	−0.2887	−0.2887	−0.2887	−0.2887	−0.2887	−0.3183
−1.0	−0.2500	−0.1649	−0.1760	−0.1753	−0.1753	−0.2500

$$-4Kb_3+g_4+\sum_{n=-\infty}^{\infty} b_{2n-3}(b_{2n-1}+b_{2n+1})=0 , \quad (4.13b)$$

$$-4Kb_{2m+1}+\sum_{n=-\infty}^{\infty} b_{2(m-n)+1}(b_{2n-1}+b_{2n+1})=0 ,$$

$$m\neq 0,\pm 1,-2 , \quad (4.13c)$$

$$\Delta g_4-2\Delta b_1 b_3-\Delta b_1^2+b_3 g_4-b_5 g_4+2b_1 b_3^2+4b_1 g_4=0 , \quad (4.13d)$$

where the constant K is given in Eq. (4.5). A full analytical solution of these equations has not been obtained. The results of a numerical solution are, however, shown in Table II and in Fig. 3. One can see that, not only is the value for the ground-state energy much improved, but the critical point $\Delta_c \approx 0.4355$ is also somewhat closer to the expected value of 1 than that in the SUB2 scheme.

We have not yet calculated the effect of including at least some of the long-range contributions of the four-body correlations. However, the expectation is that their inclusion will alter the critical behavior. Specifically, the inverse-square-law algebraic decay of the two-body coefficients b_r of Eq. (4.8) at the critical point may change to a different power-law behavior. It would be interesting to observe this phenomenon.

V. GROUND-STATE ENERGY IN 2D

In this section we focus on the 2D model on a square lattice. As in the previous section, we study the various approximation schemes separately.

A. SUB*n* scheme

The 2D full SUB2 equation is similar to Eq. (4.1) for 1D, except that the vectors r joining sites on one sublattice to those on the other are now two dimensional, i.e., $\mathbf{r}=\mathbf{r}_{ji}=\mathbf{r}_j-\mathbf{r}_i$. For simplicity we still use the symbol r instead of $\mathbf{r}$ unless it is necessary to do otherwise. Hence, the equation of the 2D SUB2 scheme can be written as

$$\sum_{\rho}\left[(1+2\Delta b_1+2b_1^2)\delta_{\rho,r}-2(\Delta+2b_1)b_r+\sum_{r'} b_{r'+\rho+\rho_1}b_{r-r'-\rho_1}\right]=0 , \quad (5.1)$$

where ρ denotes the four nearest-neighbor lattice vectors on the 2D square lattice and ρ_1 is any one of them.

One can define a sequence of partial SUB2-m approximations, similar to the 1D case. The lowest-order approximation, SUB2-2, which retains only the first two-body coefficient b_1, gives the equation

$$1-6\Delta b_1-5b_1^2=0 \quad (5.2)$$

with solution

$$b_1=\tfrac{1}{5}(\sqrt{9\Delta^2+5}-3\Delta) . \quad (5.3)$$

The full 2D SUB2 equation (5.1) can also be exactly solved as in the 1D case. The details are again given in Appendix A. The solution is given by the following equation:

$$b_r=\frac{K}{\pi^2}\int_0^{\pi}dq_x\int_0^{\pi}dq_y\frac{\cos(r_x q_x)\cos(r_y q_y)}{\gamma(\mathbf{q})}\times[1-\sqrt{1-k^2\gamma^2(\mathbf{q})}] , \quad (5.4)$$

where the constants K and k are given exactly the same as in 1D by Eq. (4.5), and the function $\gamma(\mathbf{q})$ is defined by

$$\gamma(\mathbf{q})\equiv\tfrac{1}{4}\sum_{\rho}\exp(i\mathbf{q}\cdot\boldsymbol{\rho})=\tfrac{1}{2}(\cos q_x+\cos q_y) . \quad (5.5)$$

The coefficient b_1 is determined self-consistently by the relation

$$b_1=\frac{K}{\pi^2}\int_0^{\pi}dq_x\int_0^{\pi}dq_y[1-\sqrt{1-k^2\gamma^2(\mathbf{q})}] . \quad (5.6)$$

Once b_1 is determined, the ground-state energy is again calculated by Eq. (3.19), with $z=4$ for the 2D square lattice. In Fig. 4 the energy is shown as a function of Δ within both the SUB2-2 ($\equiv$LSUB2) and full SUB2 schemes. Both approximations give the same asymptotic behavior for the energy at large Δ,

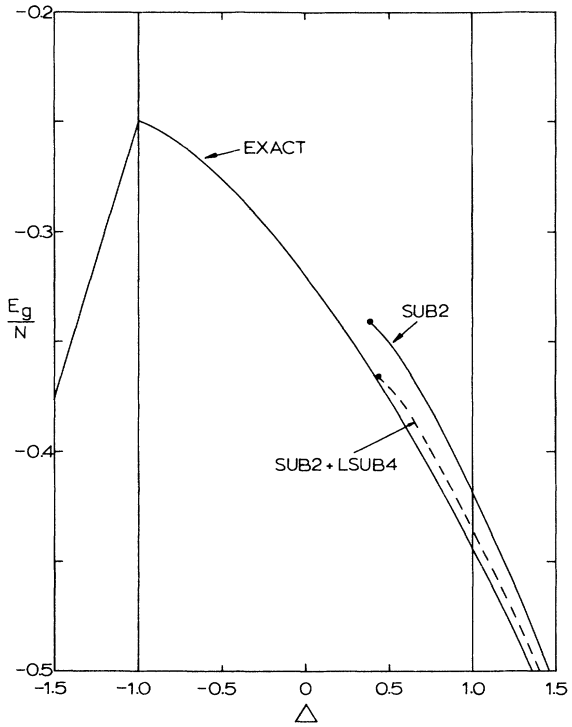

FIG. 3. Ground-state energy per spin for the 1D spin-$\frac{1}{2}$ XXZ model, showing the full SUB2 and SUB2+LSUB4 results described in the text, together with the exact results of Ref. 22. The terminating points of both CCM approximations are indicated.

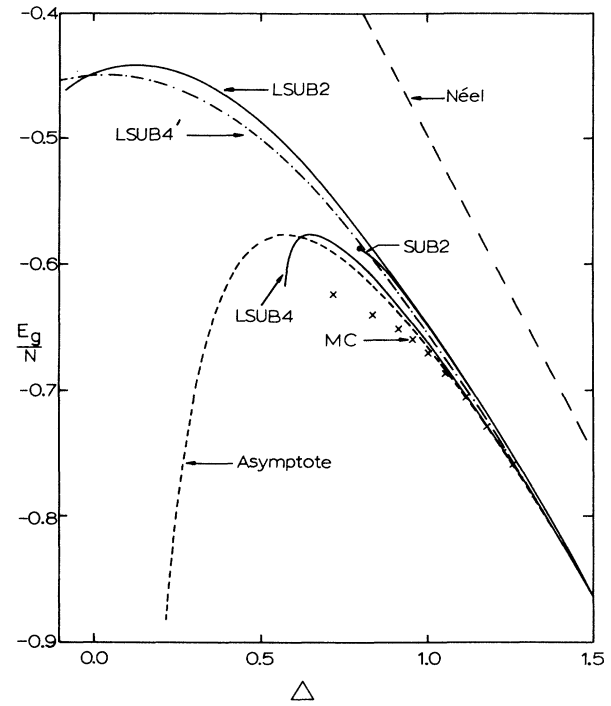

FIG. 4. Ground-state energy per spin for the 2D spin-$\frac{1}{2}$ XXZ model on a square lattice as a function of Δ, showing our LSUB2, LSUB4', LSUB4, and full SUB2 results described in the text. The terminating point of the full SUB2 scheme is indicated. Also shown are the $\Delta \rightarrow \infty$ asymptotic form of Eq. (5.7), and the Monte Carlo (MC) results of Ref. 32 (indicated by crosses).

$$\frac{E_g}{N} \rightarrow -\frac{1}{2}\left[\Delta + \frac{1}{3\Delta}\right], \quad \Delta \rightarrow \infty \ , \tag{5.7}$$

which again coincides with the exact result within the same order from perturbation theory,[31] as in the 1D case. This asymptotic behavior and the results of a recent Monte Carlo calculation[32] are also shown in Fig. 4. The numerical values for the ground-state energy in the SUB2-2 and full SUB2 approximations at $\Delta = 1$ are given in Table IV, together with other approximations for comparison.

The critical point of Eq. (5.4) is determined exactly as in 1D, i.e., by Eq. (4.7), but with a different value for α. For the square lattice we obtain numerically $\alpha \approx 0.2310$, giving $\Delta_c \approx 0.7985$, and the ground-state energy at this critical point, $E_g/N \approx -0.5837$. One sees that this value of Δ_c is much closer to the classical value of 1 than that in 1D.

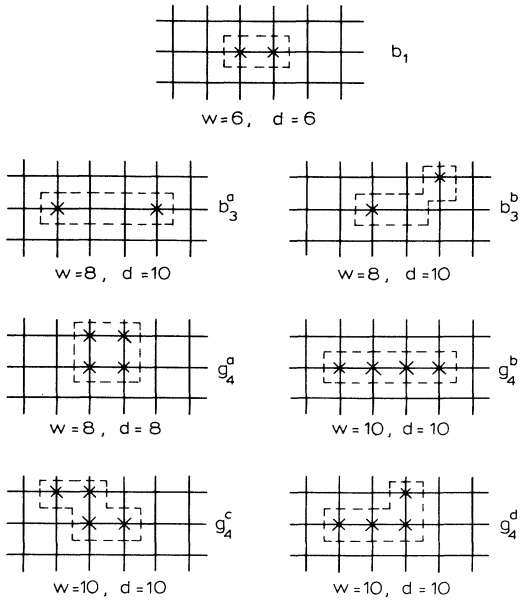

FIG. 5. A graphic illustration of the seven configurations retained in the 2D LSUB4 scheme described in the text. The crosses indicate the flipped spins with respect to the model Néel state and the dashed lines delineate the locale of the corresponding configurations. The weights w and d, defined in the text, are given, respectively, for each configuration.

B. LSUBn scheme

As in 1D, the LSUB2 approximation is the same as the SUB2-2 approximation, which is given by Eqs. (5.2) and (5.3). However, in general, the 2D case is more complicated because there are many more configurations than in 1D. For example, in the LSUB4 approximation for the 2D square lattice, there are seven independent configurations with coefficients defined as shown graphically in Fig. 5.

It is natural to expect that some of these configurations are more important than others, at least in the regime where the quantum fluctuations have not completely destroyed the classical LRO which is present in the model Néel state. We consider two possible physical measures of how important a given configuration is. The first of these is simply the number w of "wrong" bonds produced by flipping spins with respect to the Néel model state. Classically, the breaking of each bond in the antiferromagnetic regime costs energy, and hence configurations with larger values of w are likely to be less important than those with smaller values of w. Secondly, an exten-

TABLE IV. Ground-state energy per spin for the 2D Heisenberg model ($\Delta = 1$) on a square lattice under various CCM approximation schemes described in the text, together with the results of the spin-wave theory (SWT) of Ref. 33, and from the Green's-function Monte Carlo (GFMC) calculations of Ref. 28.

SUB2-2	SUB2	LSUB4'	SUB2+g_4^a	LSUB4	SWT	GFMC
−0.648	−0.651	−0.653	−0.656	−0.664	−0.658	−0.669

sion of the seemingly important concepts in 1D of locale size and the number of kinks present, leads us to consider the length, d, of the "domain boundary" of a given configuration. This is defined to be the number of lattice bonds crossed by the shortest-path circuit (indicated in Fig. 5 by the dashed lines) which encloses all of the flipped spins. The weights w and d for each of the LSUB4 configurations are indicated in Fig. 5.

From their weight numbers (w and d), one sees that b_1 is most important, followed by g_4^a, then b_3^a and b_3^b, then g_4^b, g_4^c, and g_4^d, etc. The seven coupled equations of the full LSUB4 scheme are given by

$$1-6\Delta b_1-5b_1^2+4(b_3^a)^2+14(b_3^b)^2+2b_1b_3^a+12b_1b_3^b+8b_3^ab_3^b+2g_4^a+2g_4^b+4g_4^c+8g_4^d=0\ , \tag{5.8a}$$

$$-8\Delta b_3^a+b_1^2+8(b_3^b)^2-8b_1b_3^a+8b_1b_3^b+g_4^b=0\ , \tag{5.8b}$$

$$-8\Delta b_3^b+3b_1^2+6(b_3^b)^2+4b_1b_3^a-2b_1b_3^b+8b_3^ab_3^b+g_4^c+2g_4^d=0\ , \tag{5.8c}$$

$$4\Delta g_4^a-4\Delta b_1^2+8b_1g_4^a+4b_1g_4^c+8b_1^2b_3^b-4b_3^ag_4^c-8b_3^bg_4^c-8b_3^bg_4^d=0\ , \tag{5.8d}$$

$$5\Delta g_4^b-\Delta b_1^2-2\Delta b_1b_3^a+8b_1g_4^b+b_3^ag_4^b+2b_3^ag_4^d-6b_3^bg_4^d+2b_1(b_3^a)^2+4b_1^2b_3^b+4b_1b_3^ab_3^b=0\ , \tag{5.8e}$$

$$5\Delta g_4^c-\Delta b_1^2-2\Delta b_1b_3^b+b_1g_4^a+8b_1g_4^c+2b_1g_4^d-b_3^ag_4^a-b_3^ag_4^d-3b_3^bg_4^d+2b_1^3+4b_1^2b_3^b+4b_1(b_3^b)^2=0\ , \tag{5.8f}$$

$$10\Delta g_4^d-2\Delta b_1^2-4\Delta b_1b_3^b+2b_1g_4^c+16b_1g_4^d-b_3^ag_4^b-b_3^ag_4^c-2b_3^ag_4^d-b_3^bg_4^b$$
$$-3b_3^bg_4^c-2b_3^bg_4^d+2b_1^3+2b_1^2b_3^a+6b_1^2b_3^b+2b_1b_3^ab_3^b+8b_1(b_3^b)^2=0\ . \tag{5.8g}$$

Solution of the full LSUB4 equations is done numerically. Using Eq. (3.19), we obtain the ground-state energy which is also shown in Fig. 4. From Eq. (5.8), if one retains only the two most highly weighted coefficients, b_1 and g_4^a, according to the above criteria, and sets all others to zero, one has a partial LSUB4 approximation which we denote as LSUB4′. Its result for the ground-state energy is also shown in Fig. 4. It is interesting to note that, in Fig. 4, the rapid downward bending of the energy curve around $\Delta=0.6$ in the LSUB4 scheme indicates a possible critical point near this region, reminiscent of the phenomenon observed in the 1D SUB2-m schemes discussed in Sec. IV and shown in Fig. 1.

The numerical values for the energy at $\Delta=1$ in the LSUB4′ and LSUB4 approximations are given in Table IV. One sees that, as far as the energy is concerned, the LSUB4′ scheme gives a better result than both the LSUB2 ($\equiv$SUB2-2) and the full SUB2 schemes, but the LSUB4 result is the lowest and it is the closest to the results from the best available numerical Green's-function Monte Carlo (GFMC) calculations.[28] Our results are also compared in Table IV with the corresponding result of Oguchi from Anderson's spin-wave theory (SWT),[33] in which the correction to the classical Néel value is calculated to the first order in inverse powers of the spin quantum number s, where $s=\frac{1}{2}$ here. Finally, we note that the completely independent and quite different GFMC calculations[28] of Carlson and of Trivedi and Ceperley are in excellent agreement with each other, with values $E_g/N=-0.6692\pm0.0001$ and -0.6692 ± 0.0002, respectively. Both values also agree well with another recent result of Singh,[31] who obtained $E_g/N=-0.6696\pm0.0003$ from a perturbation theory calculation performed around the Ising limit.

C. SUBn+LSUBm scheme

Just as in the case of 1D, one can take partial four-body correlations into account by including some four-body coefficients, in addition to the full SUB2 coefficients. Here we consider SUB2+g_4^a. One has three equations

$$1-6\Delta b_1-14b_1^2+\sum_{r',\rho}b_{r'}b_{r'+\rho+\rho_1}+2g_4^a=0\ , \tag{5.9a}$$

$$8(\Delta+2b_1)b_r-\sum_{r',\rho}b_{r-r'-\rho_1}b_{r'+\rho+\rho_1}=0,\quad |\mathbf{r}|\geq 3\ , \tag{5.9b}$$

$$\Delta g_4^a-\Delta b_1^2+2b_1g_4^a+2b_1^2b_3^b=0\ , \tag{5.9c}$$

where, as before, ρ_1 is any one of the four nearest neighbors of the square lattice. In particular, the critical point is now at $\Delta_c\approx0.8186$, again as in 1D closer to the value 1 than the corresponding SUB2 result. The ground-state energy at $\Delta=1$ is also given in Table IV.

VI. BRA STATE, CORRELATION FUNCTION, AND STAGGERED MAGNETIZATION

In order to calculate any physical quantities other than the ground-state energy in the CCM, the bra state is also needed. As stated in Sec. I, one of the key features of the CCM is that the bra state is not manifestly the Hermitian conjugate of the corresponding ket state in any finite CCM approximation and needs to be calculated separately. Accordingly, the CCM does not give an upper bound for the ground-state energy. However, the CCM calculation of physical values at *any level* of truncation is consistent with the important Hellmann-Feynman theorem.[34] As Thouless[35] has shown, this implies that the expectation value of any physical quantity involves the same set of diagrams as for the energy, but in which each one of the interaction potential lines is replaced one at a time by the operator whose expectation value is to be calculated.

There are two distinct versions of the CCM for

parametrizing bra states, namely, the normal CCM (NCCM) and extended CCM (ECCM) schemes. Here we use the NCCM scheme. For more detailed discussions on the parametrization of bra states within the CCM, and of the alternative ECCM scheme, the interested reader is referred to Refs. 6 and 8.

The normal CCM bra ground-state wave function $\langle\tilde{\Psi}|$ corresponds to the ket state $|\Psi\rangle$, and is parametrized by

$$\langle\tilde{\Psi}|=\langle\Phi|\tilde{S}e^{-S}\ , \tag{6.1}$$

where the correlation operator $\tilde{S}$ is built wholly out of destruction operators with respect to the model state $|\Phi\rangle$. Note that e^{-S} is clearly not equal to $e^{S^\dagger}$, where $S^\dagger$ is the Hermitian adjoint of operator S, and hence the need for the additional operator $\tilde{S}$. In our spin models on a bipartite lattice, it is given by

$$\tilde{S}=1+\sum_{n=1}^{N/2}\tilde{S}_{2n} \tag{6.2}$$

with

$$\tilde{S}_{2n}=\frac{1}{(n!)^2}\sum_{i_1,i_2,\ldots,i_n}\sum_{j_1,j_2,\ldots,j_n}\tilde{\mathcal{S}}_{i_1i_2\ldots i_n;j_1j_2\ldots j_n}\sigma_{i_1}^-\sigma_{i_2}^-\ldots\sigma_{i_n}^-\sigma_{j_1}^-\sigma_{j_2}^-\ldots\sigma_{j_n}^-\ , \tag{6.3}$$

where, as in the previous sections, the indices i and j denote the two sublattices, respectively. We note that the particular value of unity for the constant term in Eq. (6.2) implies the manifest normalization

$$\langle\tilde{\Psi}|\Psi\rangle=\langle\Phi|\Psi\rangle=\langle\Phi|\Phi\rangle=1\ . \tag{6.4}$$

By analogy with the ket state case discussed previously, the Schrödinger equation for the ground bra state is written as

$$\langle\tilde{\Psi}|H=E_g\langle\tilde{\Psi}|\ , \tag{6.5}$$

and the equations for the bra state coefficients $\tilde{\mathcal{S}}_{i_1\ldots i_n;j_1\ldots j_n}$ are found by taking the inner products of Eq. (6.5) with the complete set of states obtained by letting arbitrary configuration creation operators act on the Néel state $|\Phi\rangle$. After a simple operator manipulation, using Eqs. (3.6) and (3.7), this leads to the equations

$$\langle\Phi|\tilde{S}e^{-S}[H,\sigma_{i_1}^+\ldots\sigma_{i_n}^+\sigma_{j_1}^+\ldots\sigma_{j_n}^+]e^S|\Phi\rangle=0,\quad n=1,2,3,\ldots, \tag{6.6}$$

where we have used the fact that S commutes with all configuration creation operators. Equation (6.6) has the form of coupled but *linear* equations for the bra state coefficients once the ket state coefficients are used as known input. Once again, the resulting equations contain only finite powers of S, since the nested commutator series again terminates after a finite number of terms.

As before, one needs to define approximation schemes to solve Eq. (6.6). Here we consider the SUB2 approximation in which $S\rightarrow S_2$ and $\tilde{S}\rightarrow\tilde{S}_2$. Setting all higher-order many-body coefficients to zero, and making use of the translational invariance, we obtain for the 1D chain and the 2D square lattice, with $\tilde{\mathcal{S}}_{i;i+r}\equiv\tilde{b}_r$,

$$\sum_\rho\left[\left[1+2(\Delta+2b_1)\tilde{b}_1-4\sum_{r'}\tilde{b}_{r'}b_{r'}\right]\delta_{r,\rho}-2(\Delta+2b_1)\tilde{b}_r+2\sum_{r'}\tilde{b}_{r'}b_{r-r'-\rho}\right]=0\ , \tag{6.7}$$

where r and r' are again vectors connecting sites on different sublattices. One can obtain the lowest-order approximation, LSUB2 (≡SUB2-2), from this equation by setting all independent coefficients to zero except b_1 and $\tilde{b}_1$. This gives

$$\tilde{b}_1=\begin{cases}\dfrac{1}{2\sqrt{\Delta^2+3}} & \text{for 1D}\ ,\\ \dfrac{1}{2\sqrt{9\Delta^2+5}} & \text{for 2D (square lattice)}\ .\end{cases} \tag{6.8}$$

The full SUB2 equation (6.7) can again be solved by the Fourier-transform technique. Details are given in Appendix B. The solutions are, for both the 1D and 2D (square lattice) cases,

$$\tilde{b}_{\mathbf{r}}=\frac{D}{4K}\int_{-\pi}^{\pi}\frac{d\mathbf{q}}{(2\pi)^d}\cos(\mathbf{q}\cdot\mathbf{r})\frac{\gamma(\mathbf{q})}{\sqrt{1-k^2\gamma^2(\mathbf{q})}}\ , \tag{6.9}$$

where the constants K and k are as defined previously in Eq. (4.5), the constant D is given by

$$D^{-1}\equiv\int_{-\pi}^{\pi}\frac{d\mathbf{q}}{(2\pi)^d}\frac{1-\gamma^2(\mathbf{q})/2}{\sqrt{1-k^2\gamma^2(\mathbf{q})}}-\frac{1}{2}\ , \tag{6.10}$$

and where the function $\gamma(\mathbf{q})$ is defined by

$$\gamma(\mathbf{q})\equiv\begin{cases}\cos q, & \text{in 1D}\ ,\\ \frac{1}{2}(\cos q_x+\cos q_y) & \text{in 2D}\ .\end{cases} \tag{6.11}$$

In Eqs. (6.9) and (6.10) the meaning of the definite integrals is given explicitly in Appendix A, Eq. (A5). It is easy to see that, as for the ket state, real solutions cease to exist in Eq. (6.9) when $k>k_c=1$ (or $\Delta<\Delta_c$). In the 1D case, this leads to the asymptotic behavior as $r\rightarrow\infty$,

$$\tilde{b}_r\rightarrow\begin{cases}O\left[\dfrac{1}{l^r}\right], & \Delta>\Delta_c\ ,\\ \dfrac{1}{2K_c}, & \Delta=\Delta_c\ ,\end{cases} \tag{6.12}$$

where the constant $\tilde{l}$ (>1) is a function of Δ and $K_c=\Delta_c+2b_1$. This behavior will be used when we discuss the possible phase transition implied by the terminating point.

After both the ket and bra states are determined we can calculate the ground-state expectation value of any physical operator within the corresponding approximations. Two important such quantities are the spin-spin correlation functions and the staggered magnetization. The asymptotic value of the magnitude of the correlation function should be equal to the square of the staggered magnetization. However, in the CCM, because of the lack of a manifest Hermitian relationship between the ket and bra states, this equality does not hold in general in any given approximation. In fact, the difference between the two is a measure of the error of the corresponding approximations, as we shall shortly see.

The spin-spin correlation functions in the CCM are given by

$$\bar{G}^{\alpha\beta}(l)\equiv\langle\sigma_i^\alpha\sigma_{i+l}^\beta\rangle = \langle\Phi|\tilde{S}e^{-S}\sigma_i^\alpha\sigma_{i+l}^\beta e^S|\Phi\rangle,\quad \alpha,\beta=x,y,z\ , \tag{6.13}$$

where l is any lattice vector. Note that this definition of the correlation function differs from the usual one [e.g., Eq. (2.11)] by a factor of $(-1)^l$ which gives a minus sign if indices i and $i+l$ pertain to sites on different sublattices, and a plus sign otherwise. This is because we have employed the rotated Néel model state in which all spins are aligned along the minus z axis. Similarly, the staggered magnetization is given by

$$M^\alpha\equiv-\frac{2}{N}\sum_i\langle\sigma_i^\alpha\rangle = -\frac{2}{N}\sum_i\langle\Phi|\tilde{S}e^{-S}\sigma_i^\alpha e^S|\Phi\rangle,\quad \alpha=x,y,z\ , \tag{6.14}$$

where the summation is over one of the sublattices, and the inclusion of the minus sign ensures that M^z is positive in our rotated Néel basis.

Under the SUB2 approximation, we obtain in both 1D and 2D,

$$[\bar{G}^{zz}(l)]_{\mathrm{SUB2}}=\begin{cases}1-4(1-\delta_{l,0})\sum_r\tilde{b}_r b_r, & \text{same sublattice}\ ,\\ 1-4\sum_r\tilde{b}_r b_r+4\tilde{b}_l b_l, & \text{different sublattices}\ ,\end{cases} \tag{6.15}$$

where, as previously, the sums on r run over all vectors joining sites on different sublattices. From this equation one sees that the SUB2 estimate for $\bar{G}^{zz}(l)$ is independent of l for spins on the same sublattice, which is an unphysical consequence of the approximation. On the other hand, for the correlation between spins on different sublattices, the asymptotics of $\bar{G}^{zz}(r)$ is determined by the product $\tilde{b}_r b_r$.

From Eq. (6.15) one can define an order parameter associated with $\bar{G}^{zz}$ as

$$\mu\equiv\bar{G}^{zz}(\infty)=1-4\sum_r\tilde{b}_r b_r\ . \tag{6.16}$$

The explicit SUB2 solutions for both 1D and 2D are given by Eq. (B13) in Appendix B. In particular, at the critical point, $\mu_c=-1$ in 1D and $\mu_c\approx0.362$ in 2D (square lattice).

For the 1D case, the asymptotic behavior of $\bar{G}^{zz}(r)$ as $r\to\infty$ is easily determined. Using Eqs. (4.8) and (6.12) we have

$$\bar{G}^{zz}(r)\to\begin{cases}\mu+\dfrac{A}{L^{2r}}, & \Delta>\Delta_c\ ,\\ \mu_c+\dfrac{B}{r^2}, & \Delta=\Delta_c\ ,\end{cases} \tag{6.17}$$

where B is constant, A and L (>1) are functions of Δ only.

The correlation functions $\bar{G}^{xx}(r)$ and $\bar{G}^{yy}(r)$ are expressed in terms of *odd* powers of the ket state and bra state coefficients in the SUB2 approximation for both 1D and 2D. Again, for the correlation between two spins on the same sublattice, they are constant. For spins on different sublattices, we obtain, combining $\bar{G}^{xx}$, $\bar{G}^{yy}$, and $\bar{G}^{zz}$,

$$\bar{G}(r)\equiv\langle\boldsymbol{\sigma}_i\cdot\boldsymbol{\sigma}_{i+r}\rangle = 2\sum_{r',r''}\tilde{b}_{r'}b_{r''}b_{r+r'+r''}-8\left[\sum_{r'}\tilde{b}_{r'}b_{r'}\right]b_r +4\tilde{b}_r b_r^2+2b_r+\tilde{b}_r+4\tilde{b}_r b_r+\mu\ . \tag{6.18}$$

At the critical point, the asymptotic value of the correlation function in 1D is nonzero, $\bar{G}_c(\infty)=-1+(1/K_c)+K_c/2$. With $K_c\approx1.363$, $\bar{G}_c(\infty)\approx0.4152$ in 1D.

In the SUB2 approximation, the staggered magnetization for both the 1D and 2D square lattice models is given by

$$M^z=1-2\sum_r\tilde{b}_r b_r,\quad M^x=M^y=0\ . \tag{6.19}$$

The explicit SUB2 solutions are given by Eq. (B14) in Appendix B. The LSUB2 approximation gives

$$M^z=\begin{cases}\dfrac{1}{3}\left[1+\dfrac{2\Delta}{\sqrt{\Delta^2+3}}\right] & \text{in 1D}\ ,\\ \dfrac{1}{5}\left[1+\dfrac{12\Delta}{\sqrt{9\Delta^2+5}}\right] & \text{in 2D}\ .\end{cases} \tag{6.20}$$

The values of M^z as a function of Δ are shown in Fig. 6 for both 1D and 2D under the LSUB2 and full SUB2 approximations, together with the exact result of Baxter[25] in 1D. In Fig. 7 we also show both $(M^z)^2$ and μ as functions of Δ, in the full SUB2 approximation, for both the 1D chain and the 2D square lattice.

From Fig. 7 it is clear that the asymptotic value of $\bar{G}^{zz}(r)$, namely, μ, is not equal to the square of M^z as mentioned earlier. However, it is very close to it except near the critical point, which suggests that the SUB2 approximation is giving a good description of the Heisenberg-Ising phase over most of its range. We also observe that, in the same order of approximation, the discrepancy between $(M^z)^2$ and μ is smaller in 2D than in 1D. This is clearly because the quantum fluctuations are more significant in 1D than in 2D.

For the SUB2 approximation in the 1D case, $M^z=0$ at $\Delta=\Delta_c$ as expected. Near the critical point, M^z has the following asymptotic form:

$$M^z \rightarrow \frac{-1}{\ln(\Delta-\Delta_c)}, \quad \Delta\rightarrow\Delta_c \quad \text{in 1D} . \tag{6.21}$$

It is clear that one cannot produce the essential singularity of the exact result of Eq. (2.13) under such a low level of approximation.

Finally, we note that in 2D at the SUB2 critical point ($\Delta=\Delta_c$), our result for the staggered magnetization is nonzero and has the value $M_c^z\approx 0.682$. This is important because we believe that the critical points in our calculations correspond to those at $\Delta=1$ for the exact case in 1D and the probable case in 2D. Therefore, our results strongly suggest that the Heisenberg antiferromagnetic model on the 2D square lattice possesses a LRO. This agrees with other calculations for the square lattice. For example, Anderson's lowest-order spin-wave theory[33] gives $M_c^z\approx 0.606$ at $\Delta=1$, while the Green's-function Monte Carlo results[28] of Carlson give $M_c^z=0.68\pm 0.02$ and those of Trivedi and Ceperley give $M_c^z=0.62\pm 0.04$ at the same point.

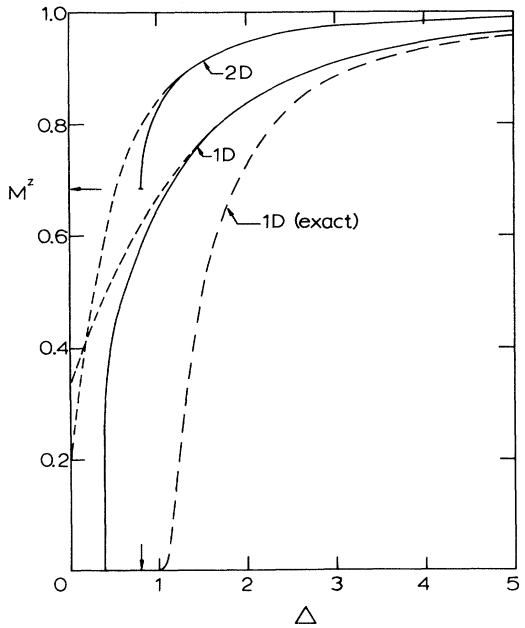

FIG. 6. Staggered magnetization M^z for spin-$\frac{1}{2}$ XXZ model in 1D and on the 2D square lattice, as functions of Δ, showing the results of the LSUB2 (dashed lines) and full SUB2 (solid lines) approximations described in the text. The exact result in 1D from Ref. 25 is also shown. The values of M_c^z and Δ_c in the full SUB2 calculation for the 2D model are indicated by arrows.

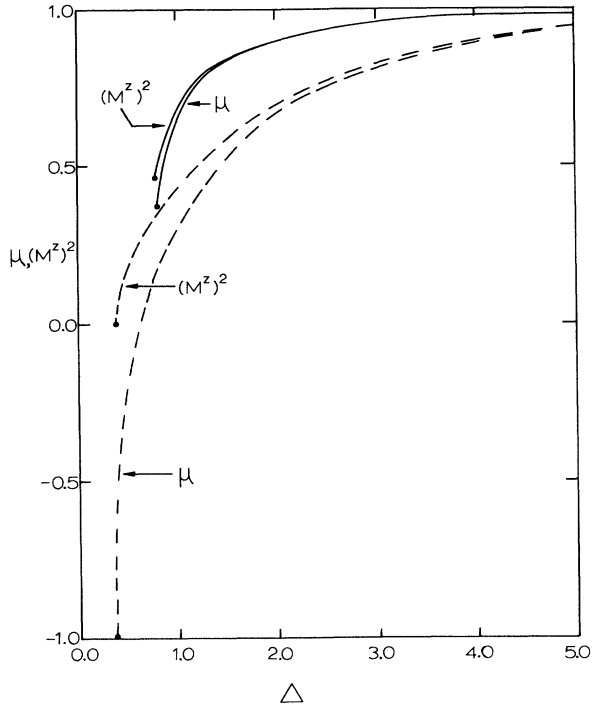

FIG. 7. The order parameter μ associated with the correlation function $\bar{G}^{zz}(r)$ and the square of the staggered magnetization M^z, as functions of Δ, showing the results of the full SUB2 scheme described in the text, for both 1D (dashed lines) and 2D (solid lines).

VII. EXCITATIONS

In this section we shall examine the excitations of our spin models within the CCM. We employ the standard CCM technique of Emrich[36] which constructs the excited ket state wave function $|\Psi_e\rangle$ in terms of a linear excitation operator X. This operator acts on the corresponding *exact* ground-state wave function so that $|\Psi_e\rangle=X|\Psi\rangle=Xe^S|\Phi\rangle$. Like the ground-state correlation operator S, X is also constructed purely from linear combinations of products of creation operators,

$$X=\sum_n X_n \tag{7.1}$$

with

$$X_n=C_n \sum_{l_1,l_2,\ldots,l_n} \mathcal{X}_{l_1 l_2\ldots l_n}\sigma_{l_1}^+\sigma_{l_2}^+\ldots\sigma_{l_n}^+ , \tag{7.2}$$

where C_n is again a suitable normalization constant.

Clearly the operator X commutes with the operator S. By using the Schrödinger equation for the excited state,

$$H|\Psi_e\rangle = E_e|\Psi_e\rangle \ ,$$

and its counterpart, Eq. (3.4), for the ground state, one readily obtains

$$e^{-S}[H,X]e^{S}|\Phi\rangle = \varepsilon_e X|\Phi\rangle, \quad \varepsilon_e \equiv E_e - E_g \ . \tag{7.3}$$

The lowest-order approximation is where $X \to X_1$, which contains only those terms with a single configuration creation operator

$$X_1 = \sum_i \mathcal{X}_i \sigma_i^+$$

or (7.4)

$$X_1 = \sum_j \mathcal{X}_j \sigma_j^+ \ ,$$

where indices i and j denote the two sublattices, respectively, as before. It is obvious that these operators produce excitations with $s^z_{\text{total}} = \pm 1$, similar to the spin-wave excitations of other theories. Higher-order approximations for the excitations with $s^z_{\text{total}} = \pm 1$ would need to include those terms in X with, for example, three creation operators such as $\sum_{i,i',j} \mathcal{X}_{ii';j} \sigma_i^+ \sigma_{i'}^+ \sigma_j^+$, etc. For the present purposes, however, we consider only the simplest approximation, given by Eq. (7.4).

The set of eigenequations for the lowest-order CCM excitation coefficients $\{\mathcal{X}_k\}$ in Eq. (7.4), where the index k runs over *either* set of sublattice vectors, is now readily obtained by taking the inner product of Eq. (7.3) with the bra states $\langle\Phi|\sigma_k^-$. We now use the SUB2 approximation for the ground ket-state correlation operator $S \to S_2$, as well as making the lowest-order approximation $X \to X_1$ for the excitation operator. For both the 1D chain and the 2D square lattice, the resulting equations take the more explicit vectorial form

$$\tfrac{1}{2}zK\mathcal{X}_{\mathbf{k}} - \tfrac{1}{2}\sum_{\boldsymbol{\rho},\mathbf{r}} b_{\mathbf{r}} \mathcal{X}_{\mathbf{k}+\mathbf{r}+\boldsymbol{\rho}} = \varepsilon_e \mathcal{X}_{\mathbf{k}} \ , \tag{7.5}$$

where, as previously, z is the coordination number of the lattice, the constant K is as defined in Eq. (4.5), the sum over $\boldsymbol{\rho}$ runs over the z nearest-neighbor lattice vectors, and the index $\mathbf{r}$ runs over all distinct lattice vectors which join sites on different sublattices. We note that Eq. (7.5) for the excitation coefficients $\{\mathcal{X}_{\mathbf{k}}\}$ is actually valid for any bipartite lattice in an arbitrary number of dimensions, just as Eqs. (5.1) and (6.7) are for the ground-state correlation coefficients $\{b_{\mathbf{r}}\}$ and $\{\tilde{b}_{\mathbf{r}}\}$, respectively.

It is trivial to verify that Eq. (7.5) has lattice plane-wave solutions,

$$\mathcal{X}_{\mathbf{k}} \to \mathcal{X}_{\mathbf{k}}(\mathbf{q}) = e^{-i\mathbf{k}\cdot\mathbf{q}}\mathcal{X}(\mathbf{q}), \quad \varepsilon_e \to \varepsilon(\mathbf{q}) \ . \tag{7.6}$$

Hence, by making use of Eq. (A4) and (A11) (with the unphysical positive sign of the square root discarded, as explained in Appendix A), we readily find that the energy dispersion relation for a $s^z_{\text{total}} = \pm 1$ plane-wave excitation of wave vector $\mathbf{q}$ is given in this lowest-order (but otherwise not truncated any further) CCM calculation, for both the 1D chain and the 2D square lattice, by

$$\varepsilon(\mathbf{q}) = \tfrac{1}{2}zK\sqrt{1-k^2\gamma^2(\mathbf{q})} \ , \tag{7.7}$$

where the function $\gamma(\mathbf{q})$ is given by Eq. (6.11), and the constants K and k by Eq. (4.5).

It is easy to see that this spectrum has a finite gap for both the 1D and 2D cases for $k^2 < 1$ or, equivalently, $\Delta > \Delta_c$. This energy gap is given by the expression

$$\varepsilon(0) = \tfrac{1}{2}zK\sqrt{1-k^2} \ . \tag{7.8}$$

The gap disappears precisely at the critical point $\Delta = \Delta_c$, where the spectrum becomes

$$\varepsilon_c(\mathbf{q}) = \tfrac{1}{2}zK_c\sqrt{1-\gamma^2(\mathbf{q})}, \quad \Delta = \Delta_c \ . \tag{7.9}$$

For the 1D chain we have $\varepsilon_c(q) \approx 1.3642|\sin q|$ with $-\pi < q \le \pi$, which may be compared with the exact result at $\Delta = 1$ quoted in Sec. II, namely, $\varepsilon(q) = \frac{1}{2}\pi|\sin q|$. We observe that the behavior of our lowest-order approximate CCM excitation spectrum, given by Eq. (7.7), very closely parallels its exact counterpart in 1D, both at and above the transition point.

However, a closer look at the asymptotes of the energy gap near the critical point reveals some differences. The asymptotic behavior of Eq. (7.8) is given in 1D by

$$\varepsilon(0) \to \text{const} \times \sqrt{\Delta - \Delta_c}, \quad \Delta \to \Delta_c \ \text{ in 1D} \ , \tag{7.10}$$

while the exact result has the essential singularity from Eq. (2.14),

$$\varepsilon(0) \to \text{const} \times \exp\left[-\frac{C'}{\sqrt{\Delta - 1}}\right], \quad \Delta \to 1^+ \ \text{in 1D} \ .$$

As in the case of the staggered magnetization, the details of this essential singularity at the critical point cannot be obtained within the SUB2 approximation, as is to be expected.

Another point is worth noting. As discussed in Sec. II, the 1D exact spin-wave spectrum of the form Eq. (2.7) is the spin-$\frac{1}{2}$ single-kink excitation. This is clearly revealed by the large-Δ limit, where one has

$$\varepsilon(q)/\Delta \to \tfrac{1}{2}, \quad \Delta \to \infty \ . \tag{7.11}$$

On the other hand, our CCM spectrum of Eq. (7.7) gives, in 1D,

$$\varepsilon(q)/\Delta \to 1, \quad \Delta \to \infty \ . \tag{7.12}$$

We realize that our excitations have spin $s^z_{\text{total}} = \pm 1$, not $\pm\frac{1}{2}$, and clearly do not correspond to the (unphysical) single-kink state of Eq. (2.7). The operator X_1 of Eq. (7.4) flips a single spin which may be regarded as creating an *adjacent* pair of kinks with respect to our approximate ground state. By contrast, the exact two-kink spectrum of Eq. (2.10) involves kinks at all possible separations, leading to a continuum of states. It seems reasonable to suppose that our spectrum corresponds to the lower boundary of this continuum, as is also believed to be the case for antiferromagnetic spin-wave theory.[37]

We now turn to the analogous discussion for the 2D case. In particular, for the 2D square lattice at $\Delta = \Delta_c$, we have the gapless spectrum

$$\varepsilon_c(\mathbf{q})=2K_c\sqrt{1-\gamma^2(\mathbf{q})}, \quad -\pi<q_x,\ q_y\leq\pi \tag{7.13}$$

with $\gamma(\mathbf{q})=\frac{1}{2}(\cos q_x+\cos q_y)$ as before. Hence, the spin-wave velocity is given by

$$v_s=2K_c=2(\Delta_c+2b_1)\approx 2.335\ . \tag{7.14}$$

By comparison with the corresponding classical spin-wave velocity, $v_0=2$ at $\Delta=1$, we have a measure of the renormalization of this quantity due to quantum fluctuations. Our value for the spin-wave velocity from Eq. (7.14) may also be compared with the GFMC result of 2.28 ± 0.1 by Trivedi and Ceperly,[28] and the value of 2.316 given by Oguchi from Anderson's spin-wave theory,[33] which again evaluates the first-order correction in inverse powers of the spin quantum number.

It is interesting to note the similarity between the spectra of the 1D and 2D models near the critical point. However, as we have discussed in Sec. VI, their corresponding staggered magnetizations have very different limiting values at the critical points that we have found, namely, zero in 1D and nonzero in 2D. It is not clear at this stage whether the 2D system really undergoes a phase transition at $\Delta=\Delta_c$ as in the case of 1D, and if so, what kind of phase transition it is. We leave further discussion to the next section.

VIII. DISCUSSION AND CONCLUSIONS

In this paper we have demonstrated the manifest success of the CCM on the spin-$\frac{1}{2}$ lattice models in 1D and 2D. Various truncation schemes have been explored, including new schemes especially tailored for these lattice systems. In particular, the LSUBn scheme includes the most important higher-order many-body corrections for a given n and gives good values for the ground-state energy of the Heisenberg-Ising phase. On the other hand, the SUBn scheme can give a phase transition due to the inclusion of certain correlations of arbitrarily long range, even at low n. The SUBn+LSUBm scheme, which combines the best features of both, has proven especially promising. The PSUBn scheme is motivated by the kink structure of the spin systems. Although this has not yet been developed in as much detail as the other schemes, we believe that it holds particular promise for a deeper study of the excited states, especially in the 1D case.

Under the SUB2 and SUB2+LSUB4 schemes, we observe a phase transition as the anisotropy varies in 1D, and possibly also in 2D. This is extremely encouraging because the CCM is an *ab initio* method which does not presuppose any knowledge of a phase transition, or any other such global behavior. It cannot, however, be expected at low levels of implementation to give a very detailed description of the actual critical behavior very close to or at the critical point. As we have seen, the essential singularity of the 1D exact results near the critical point was not produced in the SUB2 approximation. However, as shown in Fig. 6, this essential singularity region is very narrow indeed, and over most of the range the SUB2 result has the correct general form. One important feature of the CCM is that it is capable of systematic improvement. We have seen that the SUB2+LSUB4 scheme not only gives better results for the ground-state energy than does the SUB2 scheme, but it also moves the critical point Δ_c closer to the expected one. We hope that the inclusion of additional contributions, using, for example, the SUB2+LSUB6 scheme, will further improve the results close to the critical point.

One interesting result from our CCM calculations is that at the critical point $\Delta=\Delta_c$, the staggered magnetization is zero in 1D but finite in 2D. While this is in agreement with the second-order phase transition of the 1D exact result mentioned in Sec. II, it is not so conclusive in 2D where no rigorous results are available, though our result within the SUB2 approximation agrees with the spin-wave theory[33] and the GFMC calculations[28] mentioned in Sec. VI. The spin-wave excitations calculated in Sec. VII certainly support the idea that there is also a phase transition at the critical point ($\Delta=\Delta_c$) for the 2D square lattice. If this is true, the phase transition in 2D would differ from the second-order phase transition in the 1D case. The same speculation about a possible phase transition has also been made in Ref. 32 and other references cited therein. Obviously, more study is needed.

The CCM will be especially useful in other nonintegrable systems such as other 2D lattices and 1D models with spin $s>\frac{1}{2}$, particularly in view of the possibility of shedding some more light on the appearance of the so-called Haldane phase for the spin-1 chain.[38] Another straightforward extension of our calculations is to include the effect of an imposed magnetic field. For example, in this case the 1D, spin-$\frac{1}{2}$ model with an applied field was also exactly solved by Bethe ansatz.[26,39] More generally, we are hopeful that relatively simple approximations for the operators S, $\tilde{S}$, and X will lead to accurate results for a wide variety of spin systems of current interest, and that these will complement the existing methods such as direct diagonalization for small N and Monte Carlo for somewhat larger N. As shown in Secs. IV and V, our results even at this stage are approaching the accuracy of the best GFMC results[28] without much significant computing effort. We believe that our results have considerable potential for further improvement. Clearly, it should also be possible to use computer algebraic methods for generating and solving the coupled nonlinear equations which lie at the core of the CCM. Indeed, we have already made some progress in this respect and the results will be reported elsewhere. Finally, for other spin systems or for other phases, different model states might be more appropriate than the Néel state used here. We are presently investigating such questions.

ACKNOWLEDGMENTS

One of us (R.F.B.) gratefully acknowledges support for this work in the form of a research grant from the Science and Engineering Research Council (SERC) of Great Britain.

APPENDIX A: SOLUTION OF THE FULL SUB2 GROUND KET STATE EQUATIONS

The equations for the CCM ground ket state coefficients retained in the full SUB2 approximation are obtained from Eq. (3.17) by setting all of the four-body cluster coefficients $\{\mathcal{S}_{ii';jj'}\}$ to zero. The translational invariance of the lattice allows us to write $\mathcal{S}_{i;i+r}\equiv b_r=b_{-r}$, where r is thus a lattice vector which joins sites on different sublattices. Hence, the full SUB2 equations take the more explicit vectorial form:

$$\sum_{\rho}\left[(1+2\Delta b_1+2b_1^2)\delta_{\rho,\mathbf{r}}-2(\Delta+2b_1)b_{\mathbf{r}}+\sum_{\mathbf{r}'}b_{\mathbf{r}'+\rho+\rho_1}b_{\mathbf{r}-\mathbf{r}'-\rho_1}\right]=0\ , \tag{A1}$$

where the sum over ρ runs over the z nearest-neighbor lattice vectors [e.g., $\rho=\pm1$ in 1D, and $\rho=(0,\pm1),(\pm1,0)$ in 2D], ρ_1 is any particular one of these vectors, and the indices $\mathbf{r}$ and $\mathbf{r}'$ run over all distinct vectors which join a site on one of the two sublattices to a site on the other. Equation (A1) holds for both the 1D chain and the 2D square lattice. Indeed, it holds for any bipartite lattice of arbitrary dimension. Here, we consider a general hypercubic lattice of dimension d, and hence with $z=2d$ nearest neighbors.

Equation (A1) may be exactly solved by the so-called sublattice Fourier-transform (SFT) method. We first divide the lattice into the two alternating sublattices, which we label with indices i and j as before. The vectors denoting the sites in the two sublattices are denoted, respectively, as

$$\begin{aligned}&\mathbf{x}_1=(n_1,n_2,\ldots,n_d),\quad \sum_{p=1}^{d}n_p=2I\ ,\\ &\mathbf{x}_j=(m_1,m_2,\ldots,m_d),\quad \sum_{p=1}^{d}m_p=2J+1\ ,\end{aligned} \tag{A2}$$

where d is the dimensionality of the hypercubic lattice, and the parameters $\{n_p\}$, $\{m_p\}$, I, and J all take arbitrary (positive or negative) integral values. The vectors $\mathbf{r}$ and $\mathbf{r}'$ in Eq. (A1) now belong to the set $\{\mathbf{r}_{ij}\}$, where $\mathbf{r}_{ij}=\mathbf{x}_i-\mathbf{x}_j$, and each such distinct vector is counted only once in the equations. One sees immediately that all such vectors $\mathbf{r}$ belong entirely to the set of j-sublattice vectors.

We now define the SFT of the j-sublattice coefficients $\{b_{\mathbf{r}}\}$ by the relation

$$\Gamma(\mathbf{q})\equiv\sum_{\mathbf{r}}e^{i\mathbf{r}\cdot\mathbf{q}}b_{\mathbf{r}}\ , \tag{A3}$$

where $\mathbf{q}=(q_1,q_2,\ldots,q_d)$, and the sum on $\mathbf{r}$ again runs over all distinct j-sublattice vectors. Equation (A3) has the usual well-known Fourier inverse relation

$$b_{\mathbf{r}}=\int_{-\pi}^{\pi}\frac{d\mathbf{q}}{(2\pi)^d}e^{-i\mathbf{r}\cdot\mathbf{q}}\Gamma(\mathbf{q})\ , \tag{A4}$$

where, for an arbitrary function $f(\mathbf{q})$,

$$\begin{aligned}&\int_{-\pi}^{\pi}d\mathbf{q}f(\mathbf{q})\\ &\equiv\int_{-\pi}^{\pi}dq_1\int_{-\pi}^{\pi}dq_2\cdots\int_{-\pi}^{\pi}dq_d f(q_1,q_2,\ldots,q_d)\ .\end{aligned} \tag{A5}$$

If we multiply Eq. (A1) by the factor $\exp(i\mathbf{r}\cdot\mathbf{q})$, and sum on the index $\mathbf{r}$ over all distinct j-sublattice vectors, we find

$$(1+2\Delta b_1+2b_1^2)\gamma(\mathbf{q})-2K\Gamma(\mathbf{q})+\frac{1}{z}\sum_{\rho}e^{-i\rho\cdot\mathbf{q}}\sum_{\mathbf{R}'}e^{i\mathbf{R}'\cdot\mathbf{q}}\sum_{\mathbf{R}}e^{i\mathbf{R}\cdot\mathbf{q}}b_{\mathbf{R}}=0\ , \tag{A6}$$

where the constant K and the function $\gamma(\mathbf{q})$ are defined by

$$K\equiv\Delta+2b_1\ , \tag{A7}$$

$$\gamma(\mathbf{q})\equiv\frac{1}{z}\sum_{\rho}e^{i\rho\cdot\mathbf{q}}=\frac{1}{d}\sum_{p=1}^{d}\cos q_p\ , \tag{A8}$$

and where we have also made the substitutions

$$\mathbf{R}\equiv\mathbf{r}-\mathbf{r}'-\rho_1,\quad \mathbf{R}'\equiv\mathbf{r}'+\rho+\rho_1\ . \tag{A9}$$

It is trivial to observe that, since the original vectors $\mathbf{r}$ and $\mathbf{r}'$ run over all distinct j-sublattice vectors, so do $\mathbf{R}$ and $\mathbf{R}'$. Thus, Eq. (A6) becomes the simple quadratic equation for $\Gamma(\mathbf{q})$,

$$(1+2\Delta b_1+2b_1^2)\gamma(\mathbf{q})-2K\Gamma(\mathbf{q})+\gamma(\mathbf{q})\Gamma^2(\mathbf{q})=0\ , \tag{A10}$$

which is trivially solved to yield the solution

$$\Gamma(\mathbf{q})=\frac{K}{\gamma(\mathbf{q})}[1\pm\sqrt{1-k^2\gamma^2(\mathbf{q})}]\ , \tag{A11}$$

where

$$k^2\equiv\frac{1+2\Delta b_1+2b_1^2}{(\Delta+2b_1)^2}\ . \tag{A12}$$

Thus, from Eq. (A4) we obtain the solution

$$\begin{aligned}b_{\mathbf{r}}=K\int_{-\pi}^{\pi}\frac{d\mathbf{q}}{(2\pi)^d}&\frac{\exp(-i\mathbf{r}\cdot\mathbf{q})}{\gamma(\mathbf{q})}\\ &\times[1-\sqrt{1-k^2\gamma^2(\mathbf{q})}]\ ,\end{aligned} \tag{A13}$$

where we have discarded the unphysical of the two solutions for $\Gamma(\mathbf{q})$ from Eq. (A11) by appealing to the fact that we require the quantum fluctuations to disappear in the Ising limit as $\Delta\to\infty$. We thus require that each of the coefficients $\{b_{\mathbf{r}}\}$ vanishes as $\Delta\to\infty$. In particular, $b_1\to0$ (and hence $k^2\to0$) in this limit, so that the oppo-

site sign of the square root is precluded in Eq. (A13). By using the fact that $\gamma(q_1,q_2,\ldots,q_d)$ is an even function of each of its arguments, Eq. (A13) may be written in the more explicit form

$$b_{\mathbf{r}}=\frac{K}{\pi^d}\int_0^{\pi}dq_1\cos(r_1q_1)\ldots\int_0^{\pi}dq_d\cos(r_dq_d)\times\frac{1-\sqrt{1-k^2\gamma^2(\mathbf{q})}}{\gamma(\mathbf{q})}\ , \tag{A14}$$

where $\mathbf{r}=(r_1,r_2,\ldots,r_d)$ and $\mathbf{q}=(q_1,q_2,\ldots,q_d)$.

Finally, by observing that $b_{\rho}\equiv b_1$ for an arbitrary choice $\mathbf{r}\rightarrow\boldsymbol{\rho}$ among the z nearest-neighbor lattice vectors, as is required by the symmetry properties of the lattice vectors under the obvious reflections and rotations, Eqs. (A8) and (A14) readily yield the self-consistency relation for the nearest-neighbor SUB2 coefficient b_1,

$$b_1=\frac{K}{\pi^d}\int_0^{\pi}dq_1\ldots\int_0^{\pi}dq_d[1-\sqrt{1-k^2\gamma^2(\mathbf{q})}]\ . \tag{A15}$$

It is apparent that real solutions only exist for the SUB2 coefficients $\{b_{\mathbf{r}}\}$ when the condition $k^2\leq 1$ is satisfied. By making use of Eqs. (A12) and (A15), this condition may readily be shown to be equivalent to $\Delta\geq\Delta_c$, where the critical value Δ_c is self-consistently determined by the same equations.

APPENDIX B: SOLUTION OF THE FULL SUB2 GROUND BRA STATE EQUATIONS

The equations for the CCM ground bra state correlation coefficients $\{\tilde{b}_r\}$ retained in the SUB2 approximation are given by Eq. (6.7). As are those for the ground ket state, these equations are valid for any bipartite lattice in an arbitrary number of dimensions. We shall consider hypercubic lattices only, with dimensionality d and hence with the number $z=2d$ of nearest neighbors. They may be written in a more explicit vectorial form as

$$\sum_{\boldsymbol{\rho}}\left[(1+2K\tilde{b}_1-4\Xi)\delta_{\mathbf{r},\boldsymbol{\rho}}-2K\tilde{b}_{\mathbf{r}}+2\sum_{\mathbf{r}'}\tilde{b}_{\mathbf{r}'}b_{\mathbf{r}-\mathbf{r}'-\boldsymbol{\rho}}\right]=0\ , \tag{B1}$$

where, as in Appendix A, the indices $\mathbf{r}$ and $\mathbf{r}'$ run over all distinct vectors which join a site on one of the two sublattices to a site on the other, and hence belong to the set of j-sublattice vectors defined in Appendix A, the sum on $\boldsymbol{\rho}$ runs over the z $(=2d)$ nearest-neighbor lattice vectors, the constant K is defined in Eq. (A7), and the constant Ξ is defined as

$$\Xi\equiv\sum_{\mathbf{r}}\tilde{b}_{\mathbf{r}}b_{\mathbf{r}}\ . \tag{B2}$$

Equation (B1) may again be solved exactly by a similar SFT technique to those employed in Appendix A. We first define the SFT of the j-sublattice coefficients $\{\tilde{b}_{\mathbf{r}}\}$ by the relation

$$\tilde{\Gamma}(\mathbf{q})\equiv\sum_{\mathbf{r}}e^{i\mathbf{r}\cdot\mathbf{q}}\tilde{b}_{\mathbf{r}}\ , \tag{B3}$$

in analogy with Eq. (A3). Its Fourier inverse yields

$$\tilde{b}_{\mathbf{r}}=\int_{-\pi}^{\pi}\frac{d\mathbf{q}}{(2\pi)^d}e^{-i\mathbf{r}\cdot\mathbf{q}}\tilde{\Gamma}(\mathbf{q})\ , \tag{B4}$$

where the integration over $\mathbf{q}$ is given by Eq. (A5). If we now multiply Eq. (B1) by the factor $\exp(i\mathbf{r}\cdot\mathbf{q})$, and sum on the index $\mathbf{r}$ over all distinct j-sublattice vectors, we find

$$(1+2K\tilde{b}_1-4\Xi)\gamma(\mathbf{q})-2K\tilde{\Gamma}(\mathbf{q})+2\gamma(\mathbf{q})\Gamma(\mathbf{q})\tilde{\Gamma}(\mathbf{q})=0\ , \tag{B5}$$

where the function $\gamma(\mathbf{q})$ is as defined in Eq. (A8). Hence, by using the solution given by Eq. (A11) for $\Gamma(\mathbf{q})$ (with the unphysical positive sign of the square root discarded, as explained in Appendix A), we readily find the solution

$$\tilde{\Gamma}(\mathbf{q})=\frac{D}{4K}\frac{\gamma(\mathbf{q})}{\sqrt{1-k^2\gamma^2(\mathbf{q})}}\ , \tag{B6}$$

where the constant k is as given previously by Eq. (A12), and the constant D is now defined self-consistently as

$$D\equiv 2(1+2K\tilde{b}_1-4\Xi)\ . \tag{B7}$$

From Eqs. (A3) and (B3), it is trivial to prove the relation

$$\Xi=\int_{-\pi}^{\pi}\frac{d\mathbf{q}}{(2\pi)^d}\tilde{\Gamma}(\mathbf{q})\Gamma(\mathbf{q})\ , \tag{B8}$$

and hence, from Eqs. (A11) and (B6),

$$\Xi=\frac{D}{4}\left[\int_0^{\pi}\frac{d\mathbf{q}}{\pi^d}\frac{1}{\sqrt{1-k^2\gamma^2(\mathbf{q})}}-1\right]\ . \tag{B9}$$

Also, by substituting $\mathbf{r}\rightarrow\boldsymbol{\rho}$ in Eq. (B4), with $\boldsymbol{\rho}$ an arbitrary nearest-neighbor lattice vector, we readily find

$$\tilde{b}_1=\frac{D}{4K}\int_0^{\pi}\frac{d\mathbf{q}}{\pi^d}\frac{\gamma^2(\mathbf{q})}{\sqrt{1-k^2\gamma^2(\mathbf{q})}}\ . \tag{B10}$$

Finally, by combining the results of Eqs. (B7), (B9), and (B10), we find the explicit solution for the constant D,

$$D^{-1}=\int_0^{\pi}\frac{d\mathbf{q}}{\pi^d}\frac{1-\gamma^2(\mathbf{q})/2}{\sqrt{1-k^2\gamma^2(\mathbf{q})}}-\frac{1}{2}\ . \tag{B11}$$

The coefficients $\{\tilde{b}_{\mathbf{r}}\}$ are thus given from Eqs. (B4) and (B6) as

$$\tilde{b}_{\mathbf{r}}=\frac{D}{4K}\frac{1}{\pi^d}\int_0^{\pi}dq_1\cos(r_1q_1)\ldots\int_0^{\pi}dq_d\cos(r_dq_d)\times\frac{\gamma(\mathbf{q})}{\sqrt{1-k^2\gamma^2(\mathbf{q})}}\ , \tag{B12}$$

where D is given by Eq. (B11), and $\mathbf{r}=(r_1,r_2,\ldots,r_d)$, $\mathbf{q}=(q_1,q_2,\ldots,q_d)$.

The SUB2 values of the order parameter μ (given by the long-range limiting value of the spin-spin correlation function) and the sublattice magnetization M^z, are hence given, respectively, from Eqs. (6.16) and (6.19) as

$$\mu=\left[1-\int_0^{\pi}\frac{d\mathbf{q}}{\pi^d}\frac{\gamma^2(\mathbf{q})}{\sqrt{1-k^2\gamma^2(\mathbf{q})}}\right]\Big/\left[\int_0^{\pi}\frac{d\mathbf{q}}{\pi^d}\frac{2-\gamma^2(\mathbf{q})}{\sqrt{1-k^2\gamma^2(\mathbf{q})}}-1\right], \tag{B13}$$

$$M^z=\left[\int_0^{\pi}\frac{d\mathbf{q}}{\pi^d}\frac{1-\gamma^2(\mathbf{q})}{\sqrt{1-k^2\gamma^2(\mathbf{q})}}\right]\Big/\left[\int_0^{\pi}\frac{d\mathbf{q}}{\pi^d}\frac{2-\gamma^2(\mathbf{q})}{\sqrt{1-k^2\gamma^2(\mathbf{q})}}-1\right]. \tag{B14}$$

[1]F. Coester, Nucl. Phys. **7**, 421 (1958); F. Coester and H. Kümmel, *ibid.* **17**, 477 (1960).

[2]J. Čižek, J. Chem. Phys. **45**, 4256 (1966); Adv. Chem. Phys. **14**, 35 (1969).

[3]J. Paldus, J. Čižek, and I. Shavitt, Phys. Rev. A **5**, 50 (1972).

[4]R. F. Bishop and K. H. Lührmann, Phys. Rev. B **17**, 3757 (1978).

[5]H. Kümmel, K. H. Lührmann, and J. G. Zabolitzky, Phys. Rep. C **36**, 1 (1978).

[6]J. S. Arponen, Ann. Phys. (N.Y.) **151**, 311 (1983).

[7]R. F. Bishop and H. G. Kümmel, Phys. Today **40(3)**, 52 (1987).

[8]J. Arponen, R. F. Bishop, and E. Pajanne, Phys. Rev. A **36**, 2519 (1987); **36**, 2539 (1987); in *Condensed Matter Theories,* edited by P. Vashishta, R. K. Kalia, and R. F. Bishop (Plenum, New York, 1987), Vol. 2, p. 357.

[9]R. J. Bartlett, J. Phys. Chem. **93**, 1697 (1989).

[10]H. G. Kümmel, in *Nucleon-Nucleon Interaction and Nuclear Many-Body Problems,* edited by S. S. Wu and T.T.S. Kuo (World Scientific, Singapore, 1984), p. 46.

[11]B. Day, Phys. Rev. Lett. **47**, 226 (1981); B. Day and J. G. Zabolitzky, Nucl. Phys. **A366**, 221 (1981).

[12]R. J. Bartlett, Annu. Rev. Phys. Chem. **32**, 359 (1981); V. Kvasnička, V. Laurinc, and S. Biskupič, Phys. Rev. C **90**, 160 (1982); K. Szalewicz, J. G. Zabolitzky, B. Jeziorski, and H. J. Monkhorst, J. Chem. Phys. **81**, 2723 (1984); A. C. Scheiner, G. E. Scuseria, J. E. Rice, T. J. Lee, and H. F. Schaefer, III, *ibid.* **87**, 5361 (1987); E. A. Salter, G. W. Trucks, and R. J. Bartlett, *ibid.* **90**, 1752 (1989).

[13]R. F. Bishop and K. H. Lührmann, Phys. Rev. B **26**, 5523 (1982); K. Emrich and J. G. Zabolitzky, *ibid.* **30**, 2049 (1984); J. Arponen and E. Pajanne, J. Phys. C **15**, 2665 (1982); **15**, 2683 (1982).

[14]J. S. Arponen and R. F. Bishop, Phys. Rev. Lett. **64**, 111 (1990); U. Kaulfuss and M. Altenbokum, Phys. Rev. D **33**, 3658 (1986); R. F. Bishop, M. C. Boscá, and M. F. Flynn, Phys. Rev. A **40**, 3484 (1989).

[15]U. Kaulfuss, Phys. Rev. D **32**, 1421 (1985); C. S. Hsue, H. Kümmel, and P. Ueberholz, *ibid.* **32**, 1435 (1985); M. Altenbokum and H. Kümmel, *ibid.* **32**, 2014 (1985); M. Funke, U. Kaulfuss, and H. Kümmel, *ibid.* **35**, 621 (1987).

[16]D. Vaknin *et al.*, Phys. Rev. Lett. **58**, 2802 (1987); K. B. Lyons, P. A. Fleury, L. F. Schneemeyer, and J. V. Waszczak, *ibid.* **60**, 732 (1988).

[17]P. W. Anderson, Science **235**, 1196 (1987).

[18]H. A. Bethe, Z. Phys. **71**, 205 (1931).

[19]M. Roger and J. H. Hetherington, Phys. Rev. B **41**, 200 (1990).

[20]R. F. Bishop, J. B. Parkinson, and Yang Xian, Phys. Rev. B **43**, 13 782 (1991).

[21]L. Hulthén, Ark. Mat. Astron. Fys. A **26**, No. 11 (1938).

[22]R. Orbach, Phys. Rev. **112**, 309 (1958); C. N. Yang and C. P. Yang, *ibid.* **150**, 321 (1966); **150**, 327 (1966).

[23]E. H. Lieb and W. Liniger, Phys. Rev. **130**, 1605 (1963); **130**, 1616 (1963); R. J. Baxter, Ann. Phys. (N.Y.) **70**, 193 (1972).

[24]J. des Cloiseaux and J. J. Pearson, Phys. Rev. **128**, 2131 (1962); J. D. Johnson, S. Krinsky, and B. M. McCoy, Phys. Rev. A **8**, 2526 (1973); L. D. Faddeev and L. A. Takhtajan, Phys. Lett. **85A**, 375 (1981).

[25]R. J. Baxter, J. Stat. Phys. **9**, 145 (1973).

[26]N. M. Bogoliubov, A. G. Izergin, and V. E. Korepin, Nucl. Phys. **B275**, 687 (1986).

[27]A. Luther and I. Peschel, Phys. Rev. B **12**, 3908 (1975).

[28]J. Carlson, Phys. Rev. B **40**, 846 (1989); N. Trivedi and D. M. Ceperley, *ibid.* **41**, 4552 (1990).

[29]K. Kubo and T. Kishi, Phys. Rev. Lett. **61**, 2585 (1988).

[30]S. Sachdev, Phys. Rev. B **39**, 12 232 (1989).

[31]D. L. Bullock, Phys. Rev. **137**, A1877 (1965); R.R.P. Singh, Phys. Rev. B **39**, 9760 (1989).

[32]T. Barnes, D. Kotchan, and E. S. Swanson, Phys. Rev. B **39**, 4357 (1989).

[33]P. W. Anderson, Phys. Rev. **86**, 694 (1952); T. Oguchi, *ibid.* **117**, 117 (1960).

[34]H. Hellmann, Acta Physicochim. USSR **I(6)**, 913 (1935); R. P. Feynman, Phys. Rev. **56**, 340 (1939).

[35]D. J. Thouless, *The Quantum Mechanics of Many-Body Systems* (Academic, New York, 1961).

[36]K. Emrich, Nucl. Phys. **A351**, 379, 397 (1981).

[37]G. Müller, H. Thomas, H. Beck, and J. C. Bonner, Phys. Rev. B **24**, 1429 (1981); G. Müller, H. Beck, and J. C. Bonner, Phys. Rev. Lett. **43**, 75 (1979).

[38]F.D.M. Haldane, Phys. Lett. **93A**, 464 (1983); Phys. Rev. Lett. **50**, 1153 (1983); I. Affleck and F.D.M. Haldane, Phys. Rev. B **36**, 5291 (1987).

[39]N. Ishimura and H. Shiba, Prog. Theor. Phys. **57**, 1862 (1977); H. Aghahosseini and J. B. Parkinson, J. Phys. C **13**, 651 (1980).